Dissertation

Impact of arterial hypertension on electrophysiological and structural arrhythmogenic atrial remodelling

submitted by

Dr. med. univ. Martin Manninger-Wünscher

for the Academic Degree of

Doctor of Philosophy (PhD)

at the

Medical University of Graz

Department of Medicine, Division of Cardiology

under the supervision of

Assoz.-Prof. Priv.-Doz. Dr. Daniel Scherr

Assoz.-Prof. Priv.-Doz. Dr. Frank R. Heinzel, PhD

2018

Statutory Declaration and Disclosures

I hereby declare that this thesis is my own original work and that I have fully acknowledged by name all of those individuals and organisations that have contributed to the research for this thesis. Due acknowledgement has been made in the text to all other material used. Throughout this thesis and in all related publications I followed the “Standards of Good Scientific Practice and Ombuds Committee” at the Medical University of Graz.

Part of this thesis has been published in *Manninger M. et al., Arterial hypertension drives arrhythmia progression via specific structural remodeling in a porcine model of atrial fibrillation. Heart Rhythm. 2018 May 23. pii: S1547-5271(18)30503-4. doi: 10.1016/j.hrthm.2018.05.016.(1)*

David Zweiker, Arne van Hunnik, Alessio Alogna, Anton J Prassl, Julia Schipke, Stef Zeemering, Birgit Zirngast, Patrick Schönleitner, Michael Schwarzl, Viktoria Herbst, Eva Thon-Gutschi, Stefan Huber, Ursula Rohrer, Jakob Ebner, Helmut Brussee, Burkert M. Pieske, Frank R. Heinzel, Sander Verheule, Gudrun Antoons, Andreas Lueger, Christian Mühlfeld, Gernot Plank, Ulrich Schotten, Heiner Post, Xi Jin, Ursula Reiter, Gert Reiter and Daniel Scherr actively contributed to the results of this thesis and the publication resulting from the thesis project. All co-authors have explicitly agreed to the use of their data in this thesis.

September 24th, 2018

Acknowledgements

PhD student Martin Manninger-Wünscher received funding from the Medical University of Graz through the PhD Program Molecular Medicine.

First, I want to thank my supervisor, Daniel Scherr, for the opportunity to work on such a great project, for his excellent mentorship and especially for his support throughout the past years. I also want to thank my co-supervisor, Frank Heinzel, for his valuable input and guidance.

Without the help of Heiner Post, Gudrun Antoons, Andreas Lueger, Gernot Plank, Arne van Hunnik and all the other collaborators, I would have never been able to finish the project including my thesis.

Finally, I want to thank my family and especially my wife Irina for tirelessly supporting me, encouraging me and keeping my back.

Table of Contents

Abbreviations and Definitions

AAD	antiarrhythmic drug
AERP	atrial effective refractory period
AF	atrial fibrillation
AF-CHF	study: The Atrial Fibrillation and Congestive Heart Failure trial
AFCL	atrial fibrillation cycle length
AFFIRM	study: Atrial Fibrillation Follow-up Investigation of Rhythm Management
AOP	aortic pressure
APD	action potential duration
APD_{90}	action potential duration to 90% repolarization
APHRS	Asia Pacific Heart Rhythm Society
bpm	beats per minute
CHA_2DS_2-VASc score	risk score composed of congestive heart failure, arterial hypertension, age, diabetes mellitus, stroke, vascular disease and female gender
CKD	chronic kidney disease
CM	cardiomyocyte
CO	cardiac output
CS	coronary sinus
CV	conduction velocity
CVP	central venous pressure
DAPI	4',6-diamidino-2-phenylindole
DOCA	desoxycorticosterone acetate
dP/dt	change of pressure over time
ECAS	European Cardiac Arrhythmia Society
ECG	electrocardiogram
EF	ejection fraction
EHRA	European Heart Rhythm Association
EMPHASIS-HF	study: The Eplerenone in Mild Patients Hospitalization and Survival Study in Heart Failure

ESC	European Society of Cardiology
FLASH	fast low angle shot
HRS	Heart Rhythm Society
HT	arterial hypertension
IVS	intraventricular septum
LA	left atrium
LAEF	left atrial ejection fraction
LV	left ventricle
LVEDD	left ventricular end-diastolic diameter
LVEDP	left ventricular end-diastolic pressure
LVEDV	left ventricular end-diastolic volume
LVEF	left ventricular ejection fraction
LVESD	left ventricular end-systolic diameter
LVESV	left ventricular end-systolic volume
LVMM	left ventricular myocardial mass
MAP	monophasic action potential
MR	mineralocorticoid receptor
MV	mitral valve
PAP	pulmonary
PEEP	positive end-expiratory pressure
PM	pacemaker
PV	pulmonary vein
PW	posterior wall
RA	right atrium
RAAS	renin-angiotensin-aldosterone system
RACE	study: Rate Control Efficacy in Permanent Atrial Fibrillation: a Comparison between Lenient versus Strict Rate Control
RAEF	right atrial ejection fraction
RAP	rapid atrial pacing
RV	right ventricle
SE	sacrifice experiment
SEM	standard error of the mean
SHR	spontaneously hypertensive rat

SOLAECE	Latin American Society of Electrophysiology and Cardiac Stimulation
TEE	transesophageal echocardiography
TGF-β1	tissue growth factor β1
TV	tricuspid valve
USD	United States Dollar
Vbc	volume before contraction
VC	vena cava
VHD	valvular heart disease
VHF	Vorhofflimmern
Vmax	end-diastolic volume
Vmin	end-systolic volume
WGA	wheat germ agglutinin

List of Figures

List of Tables

Abstract in German

Vorhofflimmern (VHF) ist die häufigste anhaltende Arrhythmie beim Menschen. VHF ist mit einem erhöhten Risiko für das Auftreten von Schlaganfällen, Morbidität und Tod assoziiert. 60-80% der Patienten mit VHF leiden an arterieller Hypertonie (HT), diese ist ein unabhängiger Prädiktor für das Auftreten von VHF und begünstigt die Progression von VHF über unbekannte Mechanismen. Ziel dieser Arbeit war es, Mechanismen zu identifizieren, über die HT einerseits das Auftreten von VHF und andererseits das Voranschreiten der Arrhythmie begünstigt.

Methoden: In einer ersten Untersuchungsreihe wurden Hausschweine mit HT, ausgelöst durch Desoxycorticosteronacetat (DOCA), mit gesunden Tieren verglichen. Hierbei wurden echokardiographische Untersuchungen, hämodynamische Messungen, elektrophysiologische Untersuchungen im rechten Atrium einschließlich Auslösbarkeit von VHF sowie histologische Analysen durchgeführt. In einer zweiten Untersuchungsreihe wurde bei Hausschweinen, bei denen VHF mittels atrialer Tachystimulation ausgelöst wurde, entweder HT mittels DOCA induziert oder sie dienten als Kontrolltiere. In diesen Tieren wurden echokardiographische Untersuchungen, hämodynamische Messungen, elektrophysiologische Untersuchungen beider Vorhöfe, dreidimensionales elektroanatomisches Mapping, hochauflösendes epikardiales Mapping und stereologisch-histologische Untersuchungen durchgeführt.

Ergebnisse: DOCA-induzierte HT führte zu konzentrischer linksventrikulärer Hypertrophie, Hypertrophie der Vorhofkardiomyozyten, reduzierter linksatrialer kontraktiler Funktion und erhöhter Auslösbarkeit von VHF.

In Tieren mit VHF und HT war eine höhere Stabilität von VHF mit einer Vorhofdilatation und -fibrose assoziiert, nicht jedoch mit erhöhter VHF-Komplexität. Diese Ergebnisse konnten mittels Computermodell verifiziert werden.

Zusammenfassung: DOCA-induzierte HT führt zu atrialer kontraktiler Dysfunktion und begünstigt das Auftreten von VHF. Bei vorhandenem VHF begünstigt DOCA-induzierte HT die Progression durch erhöhte Stabilität der Arrhythmie durch frühes strukturelles Remodelling, welches durch Vorhofdilatation und -fibrose charakterisiert ist.

Abstract in English

Atrial fibrillation (AF) is the most common sustained arrhythmia in humans and is associated with an increased risk of stroke, morbidity and death. Arterial hypertension (HT) is found in 60-80% of AF patients, is an independent predictor of new-onset AF and contributes to AF progression via unknown mechanisms. We aimed to investigate by which mechanisms HT facilitates AF development and favours AF progression.

Methods: Two experimental series were conducted. First, landrace pigs with desoxycorticosterone acetate (DOCA) induced HT were compared to control animals. Transthoracic echocardiography, basic hemodynamic measurements, right atrial invasive electrophysiologic studies including AF inducibility testing as well as histological analyses were performed.

In a second experimental series, landrace pigs with rapid atrial pacing (RAP) induced AF were either subjected to DOCA or used as controls. In these animals, transthoracic echocardiography, basic hemodynamic measurements, left and right atrial invasive electrophysiological studies, 3D electroanatomic mapping, high density epicardial multielectrode array mapping as well as histological stereological analyses were performed.

Results: DOCA-induced HT leads to concentric left ventricular hypertrophy, atrial cardiomyocyte hypertrophy, impaired left atrial contractile function, each favouring AF inducibility.

In animals subjected to AF+HT, longer AF durations were associated with atrial dilatation and fibrosis but not with an increased AF complexity. This finding could be verified in a computational model.

Conclusion: DOCA-induced HT increases atrial susceptibility towards fibrillation at a state of impaired left atrial contractile function. In the presence of AF, DOCA-induced HT favours AF progression by increasing AF stability by early structural remodelling including atrial dilatation and fibrosis.

1 Introduction

1.1 Atrial Fibrillation

1.1.1 Definition

AF is the most common sustained arrhythmia in humans and is associated with an increased risk of stroke, morbidity and death.(2) During AF, the heart's atria beat irregularly and chaotically resulting in palpitations, shortness of breath and weakness.

1.1.2 Epidemiology

Six million individuals or 1-2% of the general population in Europe are affected by AF. The prevalence is believed to double or triple within the next 50 years.(3) According to the Framingham and Rotterdam study, the risk for individuals older than 40 years to develop AF is 1:4.(4, 5) The rise in prevalence is 1 per mil per year in 55-59 year-olds and 21 per mil per year in 80-84 year-olds.(6) AF is at risk of becoming an epidemic.

1.1.3 Morbidity and mortality

AF increases the stroke risk five-fold and one in five strokes is caused by AF.(7) In AF-caused strokes, neurological damages are significantly severer than in atherosclerosis-caused strokes.(8) AF increases the risk to develop heart failure three-fold and hospitalization risk two-to-three-fold.(9-11)

Data from epidemiological studies suggest that the presence of AF doubles death rates in affected individuals, regardless of other cardiovascular comorbidities.(11, 12) On the other hand, AF worsens outcome in patients with myocardial infarctions

and heart failure patients. The AFFIRM trial showed that successful maintenance in sinus rhythm was associated with increased survival.(13) However, controlled trials such as AFFIRM, AF-CHF, RACE have shown, that death rates are not affected when antiarrhythmic drugs are used to maintain sinus rhythm.(13-15)

1.1.4 Economic relevance of atrial fibrillation

One percent of the public insurance's health budget in Western Europe and North America are spent on the therapy of AF and its causes. In 2005, the United States of America spent 6.65 billion USD on the treatment of AF.(16) Management of AF is not only a medical, but also economic challenge of the future.

1.1.5 Associated conditions

Around 90% of patients with AF have concomitant diseases or conditions like arterial hypertension, heart failure or diabetes mellitus.(17) These factors contribute to atrial remodelling by altering ion channel function, calcium homeostasis, cell size, fibrosis and atrial structure. These changes may be involved in the initiation as well as perpetuation of AF. Understanding how exactly each concomitant disease contributes to disease initiation and progression is one of the unmet challenges in understanding the physiology of AF.

1.1.5.1 Arterial hypertension

Arterial hypertension is a risk factor for stroke in patients with AF. Elevated blood pressure enhances stroke risk, bleeding events and recurrent AF episodes. Blood pressure control is one of the key aspects in AF therapy.(18) Structural remodelling and AF recurrences can be prevented by renin-angiotensin-aldosterone system (RAAS) inhibition.(19, 20) In patients with heart failure or left ventricular hypertrophy, RAAS inhibition was associated with a lower incidence of new-onset AF.(21, 22)

These studies emphasize the importance of blood pressure control in AF patients, showing that antihypertensive therapy may also have antiarrhythmic effects.

1.1.5.2 Diabetes mellitus

Many patients with diabetes develop AF, coexistence is due to similar risk factors.(23-28) Treatment with metformin is associated with decreased long-term risk of AF and decreased long-term stroke risk, while intensive glycaemic control does not reduce new-onset AF.(29-31)

1.1.5.3 Obesity

Obesity is an important risk factor for the development of AF, prevalence increases with increasing body mass index.(32-36) Described pathomechanisms include LV diastolic dysfunction, higher sympathetic activity, inflammation and atrial fatty infiltration.(37-39) In these patients, weight reduction, management of other cardiovascular risk factors and improvement in cardiorespiratory fitness can decrease AF burden, AF recurrences and symptoms.(40-43)

1.1.5.4 Aging

Epidemiological studies have shown the odds ratio of developing AF is 2.1-2.2 for each decade of advancing age.(44) It is unclear, whether accumulation of cardiovascular risk factors might be a confounding factor accounting for this increasing risk. Several animal studies have shown that the ageing heart develops structural characteristics that predispose to develop AF such as interstitial fibrosis and connexin remodelling.(45-49)

1.1.5.5 Heart failure

Many patients with heart failure develop AF, both entities share similar pathophysiology and risk factors.(50-53) AF patients who suffer from heart failure with preserved or reduced ejection fraction have a worse prognosis including increased mortality.(54-57) The general therapeutic approach in AF patients with or without heart failure does not differ, but anticoagulation is one of the few therapeutic approaches that enhances prognosis.(58)

A multicentre randomized controlled study in 179 patients could show that catheter ablation of AF in patients with heart failure with reduced ejection fraction under optimal medical therapy reduced mortality significantly.(59) Since rhythm control with antiarrhythmic drugs is not superior to rate control in patients with heart failure and AF, this study shows that alternative methods of rhythm control therapy can improve prognosis.(14)

1.1.5.6 Valvular heart disease

Around one third of patients with AF have some form of valvular heart disease (VHD).(12, 60, 61) VHD is an independent predictor of new onset AF.(62) In patients with severe VHD as well as patients undergoing surgery or transcatheter interventions for aortic or mitral valve disease, AF worsens the prognosis.(63) AF and VHD interact with each other by pressure and volume overload, tachycardia and neurohumoral activation.(64-69)

1.1.5.7 Obstructive sleep apnoea

AF is associated with obstructive sleep apnoea.(70, 71) Potential pathomechanisms involved in AF development are autonomic dysfunction, hypoxia, hypercapnia and inflammation.(17, 70-73) Therapy of obstructive sleep apnoea by positive pressure ventilation may reduce AF recurrence.(74-77)

1.1.5.8 Chronic kidney disease

15-20% of patients with chronic kidney disease (CKD) suffer from AF.(78) Deterioration of renal function is frequent in patients with AF and has to be monitored in order to avoid overdosing of anticoagulants or antiarrhythmic drugs.(79)

1.1.6 Progression of atrial fibrillation

The natural time course of the disease is often characterized by short and rare episodes in the beginning (paroxysmal), which evolve to more stable and frequent episodes. This progression is favoured by risk factors like arterial hypertension, vascular disease, heart failure, valvular disease, diabetes mellitus or thyroid dysfunction.(12, 60, 80) After years, most patients will develop sustained forms of AF (persistent or permanent). Overall progression rate from paroxysmal to persistent or permanent AF is around 60% for all AF patients, while it is significantly lower for patients without risk factors (lone AF).(2, 81, 82)

1.1.7 Classification and development of atrial fibrillation

The exact mechanisms of AF development remain unclear. Many patients with numerous risk factors associated with AF never develop AF throughout their lifetime, while some patients develop AF without any predisposing risk factors.(2)

Before 2014, AF was described as “acute” or “chronic” with respect to the temporal nature of the arrhythmia. In recent guidelines, AF is classified as paroxysmal, persistent, long-standing persistent and permanent.(2, 83) Paroxysmal AF terminates spontaneously or with an intervention within seven days of onset. If AF fails to self-terminate within seven days or if rhythm control therapy is initiated after an AF duration of longer than seven days, it is classified as persistent. If AF lasts longer than 12 months, but rhythm control strategy is adopted, it is classified as

long-standing persistent. Permanent AF is used to describe patients, in whom a decision was made to no longer pursue rhythm control therapy.

Subclinical AF describes patients, in whom AF was detected by cardiac monitoring from implantable devices but who are asymptomatic.(2)

In paroxysmal AF, triggers like ectopic beats from the pulmonary veins, atrial premature beats or episodes of atrial tachycardia may initiate the arrhythmia and thereby largely contribute to the early progression of the disease. During the development to permanent AF, the substrate gains in importance over the initiating triggers.(84) Recurrent episodes of AF lead to specific forms of atrial remodelling (electrical, structural, ultrastructural) favouring arrhythmia stability (AF begets AF).(85)

1.1.8 Substrate remodelling in atrial fibrillation

Substrate remodelling during the development and progression of AF consists of the early electrical remodelling caused by recurrent episodes of AF or atrial tachycardia, which is characterized by shortening of the action potential duration (APD), shortening of the effective atrial refractory period (AERP) and loss of rate adaption of the AERP as well as a “second factor” that is most likely related to structural atrial remodelling.(85, 86) Fibrosis, cardiomyocyte hypertrophy, changes in atrial architecture (dilation, altered composition of the extracellular matrix, endo-epicardial dissociation) and rearrangement of connexins are some of the described structural changes that may contribute to the development of AF.(17, 87) Cardiovascular risk factors favour transition from paroxysmal to persistent AF by accelerating structural remodelling and/or increasing complexity of the substrate.(17) In experimental models of AF, structural changes were associated with an increase in AF complexity during the progression of AF.(88) AF complexity (complexity of fibrillatory conduction during AF) is assessed by multielectrode mapping of activation during episodes of AF and is thought to increase during

progression of the arrhythmia and has therefore been widely used for quantification of the degree of electrophysiological alterations in the atria.(88-90)

One of the ultrastructural changes observed in AF progression is rearrangement of epicardial and endocardial bundles leading to dissociation of endo- and epicardial electrical activity creating a 3-dimensional AF substrate.(89) Due to the invasiveness of the used methods, simultaneous mapping of both endo- and epicardium is currently restricted to animal models.

Spatially discordant action potential duration (APD) alternans favours the development of AF by creating areas of repolarization dispersion.(91) APD alternans is a marker for altered calcium handling and may explain transition from pacing, atrial flutter or pulmonary vein ectopy to AF.(92-94) Measurements of monophasic action potentials (MAP) to determine APD can be performed in vivo using special catheters which can be used to characterize the atrial substrate.

However, while extensive research has been conducted to describe the “second factor” besides electrical remodelling that contributes to AF progression, it is not known how exactly the proposed structural and ultrastructural changes affect atrial conduction. A promising integrative approach is combining observations from patients and animal models and computer simulations using mathematical electrophysiological models.(95)

1.1.9 Therapy of atrial fibrillation

Every patient who is diagnosed with AF should be evaluated for his or her individual stroke risk. The CHA_2DS_2-VASc score provides a useful tool to estimate this risk. It includes specific risk factors that are associated with an increased stroke risk such as arterial hypertension (1 pt.), congestive heart failure (1 pt.), age (65-74: 1 pt., $\geq$75: 2 pts), prior transient ischemia attack or stroke (2 pts), vascular disease (1 pt.) and female gender (1 pt.). Annual stroke risk from 0 to a maximum of 9 points is 0, 1.3, 2.2, 3.2, 4, 6.7, 9.8, 9.6, 6.7, 15.2 %, respectively.(2)

The two therapeutic approaches in AF therapy are rate and rhythm control therapy. A rate control therapy uses drugs that slow atrioventricular conduction such as beta

blockers, calcium channel blockers or digoxin. Target heart rates depend on the patient's symptoms.(2)

Rhythm control strategy is defined by the goal of restoring sinus rhythm. This can be achieved by class I or III antiarrhythmic drugs, electrical cardioversion, catheter ablation or surgical ablation.(2)

Since the first description of triggers from pulmonary veins that initiate AF in 1998, catheter ablation has developed to a common treatment to prevent AF.(2, 96-98) The primary goal of catheter ablation in patients with paroxysmal AF is to isolate the pulmonary veins from the atria, which does not suppress pulmonary vein ectopy, but prevents these ectopies from inducing AF. Ablation has shown to be more effective than antiarrhythmic drug therapy in maintaining sinus rhythm and has complication rates comparable to those under antiarrhythmic drug therapy.(99, 100) Recent ESC guidelines and HRS/EHRA/ECAS/APHRS/SOLAECE consensus statement recommend catheter ablation to improve symptoms in patients with symptomatic AF recurrences despite antiarrhythmic drug (AAD) therapy.(2, 98) Considering patient choice as well as benefit and risk of an invasive treatment, catheter ablation can be considered as a first-line therapy before starting AAD therapy.

While pulmonary vein isolation is the cornerstone of AF ablation, success rates in patients with persistent AF remain disappointing. This might be due to the fact that with progression of the arrhythmia, the atrium undergoes electrical and structural remodelling and pulmonary vein triggers lose importance in AF pathophysiology.(84) More extensive ablations such as a stepwise approach with additional lines on the atrial roof and mitral isthmus, ablation of complex fractionated atrial electrograms, rotor ablation, isolation of the left atrial appendage or box isolation of low voltage areas have been proposed, but randomized controlled trials are either disappointing or missing.(101-108)

The disappointing results in rhythm control therapy in patients with progressed AF may be explained by the incomplete understanding of the mechanisms favouring progression of the arrhythmia.(95, 109)

1.1.10 Animal models of atrial fibrillation

Since animal models of AF should be a mimicry of the clinical AF phenotype, various models have been developed using pathogenetic factors associated with human AF. These include atrial tachycardia, heart failure, arterial hypertension, mitral valve disease, and acute volume overload.(110)

1.1.10.1 Atrial tachycardia

A common method to study the effect of recurrent episodes of AF or atrial tachycardia on the progression of the arrhythmia is the use implanted pacemakers allowing atrial tachypacing.(88, 111-116) These models are characterized by progressive electrical remodelling including shortening of the AERP, which differs between the animal used.(17) Atrial tachypacing using implantable pacemakers requires large animals such as dogs, goats, pigs or sheep.(110)

1.1.10.2 Atrial structural remodelling

Ventricular tachypacing is used in dogs or sheep to induce congestive heart failure, creating a substrate for AF.(117-119) Experimental models of congestive heart failure do not show changes in AERP or global conduction velocity, while high-density mapping suggests that focal activations originate from the pulmonary vein regions in these models. However, it is unclear how this pulmonary vein activity maintains AF.(120)

Induction of mitral regurgitation by transoesophageal echocardiography (TEE) guided catheter-guided avulsion of chordae in dogs results in a substrate for the development of AF.(121) Volume overload of the left atrium leads to interstitial fibrosis and chronic inflammation.(122) Refractory periods are increased and conduction velocities are slowed leading to a higher susceptibility to AF.(121, 123)

Open heart surgery is associated with the development of AF, while sterile pericarditis is believed to contribute to rendering atrial more susceptible to AF. Inducing sterile pericarditis in dogs results in higher incidence of sustained AF.(124)

Induction of an atrioventricular block in goats leads to progressive atrial dilatation and prolonged AF. Refractory periods and AF cycle length remain constant in this model, while atrial hypertrophy without fibrosis develops over the observed time period of four weeks.(125)

Volume overload is used to induce chronic atrial dilatation and persistent AF. This overload is achieved by creating aortic-to-left atrium shunts in goats, aorto-pulmonary shunts in sheep or arteriovenous shunts in rabbits.(126-128) All of these models are characterized by atrial dilatation and higher stability of AF, while changes in refractory periods, conduction velocities and ultrastructure vary.

1.1.10.3 Acute atrial stress

Some models use acute stress to promote AF without chronic alterations in atrial structure and function.(110) These models are frequently used for the evaluation of antiarrhythmic drugs.

In isolated rabbit hearts without pericardium, acute pressure overload leads to shortening of AERP and increased susceptibility to AF.(129) Development of AF relies on atrial stretch and can be suppressed by blocking agents of stretch-activated agents.(129-132)

Aconitine opens cardiac sodium channels causing triggered activity and the development of AF. This model was used to study antiarrhythmic agents such as tertiapin and NIP-151.(133, 134)

Coronary artery disease is an important risk factor for the development of AF, while the underlying mechanisms remain unclear. Selective atrial ischemia was used in dogs to increase duration of AF.(135) Results from this model reveal that ischemia acute atrial ischemia in the presence of coronary artery disease may be an important pathomechanism with a specific therapeutic profile.

1.1.10.4 Autonomic models

Vagal nerve stimulation induces AF and is used in dogs or sheep to screen for potential antiarrhythmic drugs.(136-138) During vagal stimulation, acetylcholine activates potassium currents, which shortens action potential duration and AERP resulting in AF.(136, 137) Alternatively, acetylcholine perfusion of Langendorff-perfused sheep hearts is used to induce AF ex vivo.(139, 140)

1.1.10.5 Rodent models

Inhibition of glycolysis in isolated hearts of old rats (28 months) induces spontaneous AF via inducing calcium handling abnormalities.(141)

Rats subjected to asphyxia have an increased inducibility of AF. Possible mechanisms include vagal or sympathetic nerve discharge.(142)

Transgenic mouse models either use genes involved in promoting conduction abnormalities or involved in calcium handling. Activation of TGF-β1, overexpression of angiotensin converting enzyme or JDP2 results in atrial fibrosis, atrial dilatation, connexin remodelling or atrioventricular block.(143-145) Overexpression of Kir2.1 or KCNE1-KCNQ1, knockout of connexin 40, $Ca_v1.3$, KCNE1, NUP155 or FKBP12.6, knock-in of RYR2-S2814A and R176Q mutation of ryanodine receptor 2 lead to electrical remodelling promoting AF.(143-154) These models are characterized by bradycardia, conduction delay, atrioventricular block, accelerated repolarization, decreased calcium currents, reduced calcium transients or impaired calcium handling. Models of dilative cardiomyopathy induced by overexpression of Rho-A, MURC or TNF-α results in atrial dilatation, atrial fibrosis, bradycardia, atrioventricular block and connexin remodelling.(155-158) Overexpression of Junctin, junctate-1, CRE modulator, HopX, Rac1 and Gaq result in a phenotype of hypertrophic cardiomyopathy with a substrate for AF characterized by atrial dilatation, fibrosis, bradycardia and decreased connexin 40.(159-164)

1.2 Arterial Hypertension

1.2.1 Definition

Arterial hypertension is a chronic condition, where blood pressure in the arteries is elevated. Usually, elevated blood pressure does not cause symptoms. However, arterial hypertension is a major risk factor for heart failure, stroke, coronary artery disease, peripheral vascular disease, loss of vision, dementia and chronic kidney disease.(165) Arterial hypertension can be classified in primary (essential hypertension) and secondary hypertension. The first is caused by genetic as well as unspecific lifestyle factors and the latter by an identifiable cause such as chronic kidney disease, renal artery stenosis or endocrine disorders.

Blood pressure is usually described in millimetres mercury (mmHg) and expressed by the systolic (maximum) and diastolic (minimum) pressures. Therapy goals for optimal blood pressure differ by age and underlying comorbidities.(165) Recent guidelines of the European Society of Cardiology define <120/<80 mmHg as optimal, 120-129/80-84 mmHg as normal, 130-139/85-89 as high normal blood pressure, 140-159/90-99 mmHg as Grade 1 Hypertension, 160-179/100-109 mmHg as Grade 2 Hypertension and ≥180/≥110 mmHg as Grade 3 Hypertension.(165)

1.2.2 Epidemiology

Overall prevalence in European countries is around 30-45% of the general population. Prevalence shows a steep increase with higher age.(166) Cross-sectional surveys showed, that screening reveals a large number of patients with high blood pressure, who receive no treatment and that a large number of patients under antihypertensive medication does not have controlled blood pressure. In May 2017, the International Society of Cardiology screened 1201570 patients in 80 countries and showed that 17.3% of people without previously known arterial hypertension were hypertensive and 46.3% of patients receiving antihypertensive drugs did not have controlled blood pressure.(167)

1.2.3 Causes

1.2.3.1 Primary Hypertension

Hypertension is a result of a complex interaction of environmental and genetic factors. Various genetic variants have been described, that are associated with elevated blood pressure.(168-170)

Arterial hypertension is associated with age, high salt intake in salt sensitive individuals and lack of exercise.(165, 171)

1.2.3.2 Secondary hypertension

Secondary hypertension is caused by an identifiable primary cause and is less common than primary hypertension (only around 5%).(165)

Hypertension may be caused by other medications such as non-steroidal anti-inflammatory drugs or steroids. Endocrine disorders such as Conn's syndrome, hyperaldosteronism, Cushing's syndrome, hyperthyroidism, hypothyroidism, hyperparathyroidism, pheochromocytoma or acromegaly cause elevated blood pressure. Chronic kidney disease as well as renal artery stenosis from fibromuscular dysplasia or atherosclerosis may also cause arterial hypertension.(165)

1.2.4 Therapy

Blood pressure targets depend on underlying conditions and should be stricter in patients with more risk factors, these being male sex, age >55 years in men and >65 years in women, smoking, dyslipidaemia, impaired fasting glucose, abnormal glucose tolerance test, obesity, family history of premature cardiovascular disease, organ damage (left ventricular hypertrophy, carotid wall thickening, carotid plaque,

high pulse wave velocity, decreased ankle-brachial index, chronic kidney disease, microalbuminuria) and diabetes mellitus.(165)

Lifestyle changes such as weight loss, physical exercise, healthy diet and decreased salt intake can lower blood pressure.(165)

Several classed of medications are available for the treatment of arterial hypertension. These include thiazide-diuretics, calcium-channel blockers, angiotensin converting enzyme inhibitors, beta blockers and mineralocorticoid antagonists. In most patients, a combination of these antihypertensive drugs is necessary to reach blood pressure goals.(165)

In case of elevated blood pressure that is resistant to lifestyle changes and antihypertensive medication, invasive approaches such as renal denervation or baroreceptor stimulation may be considered.(165)

1.2.5 Animal models of arterial hypertension

Since animal models of arterial hypertension should mimic hypertension in humans, various models have been developed using pathogenetic factors associated to human hypertension. These include genetic predisposition, excessive salt intake and hyperreactivity of the renin-aldosterone-angiotensin system.(172)

1.2.5.1 Genetic hypertension

The most commonly used model for hypertension research are spontaneously hypertensive rats (SHR). These are developed by inbreeding Wistar rats with the highest blood pressure. Blood pressure increases after 4 weeks and reaches around 180 mmHg at week 6.(172, 173) SHR may develop cardiac hypertrophy, heart failure and kidney disease.(174-176)

Dahl salt-sensitive rats are derived from Spraque-Dawley rats that undergo high-salt diet.(177) Normal salt diet leads to hypertension in Dahl salt-sensitive rats,

which develop cardiac hypertrophy, heart failure and hypertensive kidney disease.(176, 178)

Transgenic mouse models are used overexpressing genes that are associated with elevated blood pressure, such as Ren-2 or TGR(mREN2)27. This results in cardiac hypertrophy and proteinuria.(179-181)

1.2.5.2 Endocrine hypertension

In 1943, Selye et al. presented a rat model using an aldosterone agonist (desoxycorticosterone acetate, DOCA) in combination with high salt diet and unilateral nephrectomy which resulted in significant arterial hypertension, hypertrophy and capsular fibrosis of the renal glomeruli as well as hyalinization and necrosis especially in the vasa afferentia.(182)

DOCA was used in multiple animal models that are characterized by cardiac hypertrophy, proteinuria, glomerulosclerosis and impaired endothelium-related relaxations.(183-185)

Kistler et al. used a sheep model of corticosterone-induced hypertension.(186) Pregnant ewes received corticosteroids intravenously at 27 days of gestation which resulted in significantly elevated blood pressure in their offspring.

1.2.5.3 Renal hypertension

Performing nephrectomy or producing renal artery stenosis by clipping of the vessel are used in various rodent models to induce secondary hypertension. These include the two-kidney one-clip, one-kidney one-clip and two-kidney two-clip models.(187, 188)

1.2.5.4 Environmental hypertension

Flashing lights, loud noises, restraint cage, cold or hot stimuli were used in rats to develop a stress-induced model of arterial hypertension.(189, 190)

1.2.5.5 Pharmacological hypertension

The use of nitric oxide synthetase inhibitors such as L-NAME leads to nitric oxide deficiency resulting in arterial hypertension, which was demonstrated in various rodent models.(191-193)

1.3 Atrial fibrillation in the presence of arterial hypertension

The most common of the above-mentioned risk factors for progression of AF is arterial hypertension. It is found in most AF patients, playing an important role in AF development and progression.(11) There is ample evidence that arterial hypertension leads to structural atrial remodelling and by this favours the development of AF and accelerate the transition from paroxysmal to permanent AF.(194, 195)

1.3.1 Experimental studies

Electrophysiological animal studies in models of hypertension are relatively rare.(17) In a sheep model with arterial hypertension induced by prenatal corticosteroid exposure, young animals had increased AF stability after atrial burst pacing, reduced atrial conduction velocities, increased fibrosis and cardiomyocyte hypertrophy.(186) In spontaneously hypertensive rats, AF inducibility and increased fibrosis were observed.(196)

Experimental data from the animal models mentioned above suggest that HT leads to early and progressive left atrial (LA) electrophysiological and structural remodelling. HT quickly leads to LA hypertrophy, fibrosis and inflammation.(196-200) Electrophysiological remodelling occurs within a few weeks and includes increased AF inducibility, atrial wavelength shortening and enhanced heterogeneity of conduction.(186, 196, 198, 201-203) LA remodelling increased with longer duration of HT.(196) Abnormalities in calcium handling are a potential trigger leading to AF.(200) Lateralisation of connexins during LA remodelling is described in many animal models and is associated with an increased propensity to tachyarrhythmias.(201, 204, 205)

The pathophysiology of arrhythmogenesis in HT is complex and includes haemodynamic changes, atrial and ventricular structural remodelling (i.e. fibrosis) and neuroendocrine factors.(206) In patients with HT, poor blood pressure control

favours the development of AF via diastolic dysfunction, elevated left atrial filling pressures and left atrial remodelling. A blunted nocturnal blood pressure fall also increases the likelihood of developing AF, possibly due to the persistently elevated left atrial filling pressures.(207) The renin-angiotensin-aldosterone system plays an important role in the development of AF in the presence of HT. Activation of AT1 receptors by angiotensin II increases synthesis of TGF-β1 and releases growth factors and mediators of inflammation (i.e. IL-6), all of which results in atrial fibrosis.(208, 209)

1.3.2 Translational aspects

Translating experimental finding to humans, several mechanisms have been described that are thought to play an important role in pathophysiology of AF in patients with HT. All changes that are thought to be involved in this pathophysiology can be subsumed as the so-called atrial cardiomyopathy.(210) This involves architectural, structural, contractile and electrophysiological changes that predispose for AF. Hemodynamic factors include increased LV stiffness, LV diastolic dysfunction and increase in LV wall thickness leading to increased LA filling pressures, LA wall thickening, LA contractile dysfunction, which again favours LA enlargement.(211) On the other hand, histological changes such as fibroblast proliferation, fibrosis, cardiomyocyte hypertrophy resulting in disorders of interconnections between cardiomyocyte bundles lead to AERP shortening, conduction blocks and re-entry.(17)

1.3.3 Human data

Epidemiological data from the Framingham study demonstrated a relationship between blood pressure and LA dilatation as well as increased risk of AF with increase in LA diameter and LV wall thickness.(212, 213) The risk of developing AF increases with age and LV mass in patients with HT.(214) LV hypertrophy is a

significant predictor of AF in hypertensive patients as well as in the general population.(215, 216)

Medi et al. performed a detailed mapping study in patients with chronically treated HT and LV hypertrophy without history of AF.(217) Right atrial (RA) electroanatomic mapping was performed and right atrial refractory periods, conduction velocities, activation times and voltages were measured in 10 patients with HT and 10 patients without HT. In this population, HT was associated with conduction slowing, an increase in low voltage areas and increased AF inducibility.

1.4 Aim

In humans, studies on interaction of specific risk factors with AF are scarce, since multiple predisposing factors for AF often coexist, making description of risk factor specific remodelling difficult. Investigation of the pathomechanisms is only possible in animal models.

We aimed to characterize electrophysiological and structural changes that promote the development and progression of AF in the presence of HT. For this, we conducted experimental series in (A) a porcine model of HT and (B) a porcine model of AF and HT.

In prior studies, we have shown that HT increased the stability of AF already after two weeks in a porcine model of right atrial tachypacing-induced AF.(218) We believe that this increased stability is attributed to a specific pattern of structural remodelling. We hypothesize that hypertension leads to increased left atrial filling pressures resulting atrial dilatation and fibrosis, enhancing the proarrhythmic potential of the substrate.

2 Materials and Methods

In order to investigate how arterial hypertension favours 1) the development and 2) the progression of AF, two experimental series were performed that are described separately.

For these experiments, we used landrace pigs, since their heart's size, anatomy and electrophysiological properties are similar to humans. Due to the complexity of combining AF with HT, we used the DOCA model for HT, since it requires only a minimally invasive operative procedure combined with a dietary intervention.

2.1 Development of atrial fibrillation in the presence of arterial hypertension

We previously established a porcine model of arterial hypertension by subcutaneous implantation of DOCA pellets (deoxycorticosterone acetate, an aldosterone analogue) and high-salt feeding.(1, 219) This model is characterized by an increase of systolic blood pressure, left ventricular concentric hypertrophy, atrial and left ventricular cardiomyocyte hypertrophy, but no overt increase of atrial and left ventricular collagen content. Importantly, animals have preserved systolic function as demonstrated by echocardiography and invasive hemodynamic measurements. On a cellular level, we found impaired cardiomyocyte contractility, which could be reversed by NCX-blockade.(220)

In a first experimental series, we sought to test whether these cellular findings are also reflected in vivo and if these changes render the atria more susceptible to AF. For this purpose, 15 animals underwent an electrophysiological study including AERP measurements and AF inducibility testing as well as magnetic resonance imaging.

In short, landrace pigs were implanted with DOCA-pellets and high-sugar and high-salt diet was started. After six weeks, a sacrifice experiment was performed including magnetic resonance imaging, an electrophysiological study as well as

tissue harvesting. Weight-matched animals served as controls. Figure 1 illustrates the experimental protocol.

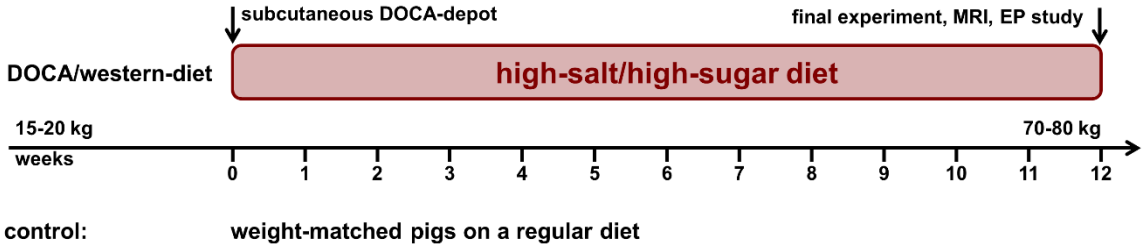

Figure 1. Scheme of the experimental protocol.

Animal handling was conforming with the Guide for the Care and Use of Laboratory Animals (National Institute of Health, USA). Experimental protocols were approved by the local Bioethics Committee of Vienna, Austria (BMWF-66.010/0108-II/3b/2010, BMWF-66.010/0128-II/3b/2012, BMWF-66.010/0091-II/3b/2013, BMWFW-66.010/0050-WF/II/3b/2014).

2.1.1 DOCA implantation

To induce arterial hypertension, 7 landrace pigs were treated with DOCA combined with a high sugar/salt/potassium diet for 12 weeks. DOCA pellets with a 90-day release (Innovative Research of America, USA) were implanted subcutaneously in the inguinal region under sedoanalgesia with ketamine (20mg/kg) and midazolam (0.25mg/kg). 8 weight-matched animals (65±4kg vs. 66±6kg) served as controls.

2.1.2 Final experiment

The experimental setup has been described before.(221, 222) Briefly, animals were fasted overnight with free access to water and sedated with 0.5 mg/kg midazolam and 20 mg/kg ketamine. After administration of 1 mg/kg propofol, the animals were intubated, and anaesthesia was maintained with sevoflurane (1%), fentanyl (35

µg/kg/h), midazolam (1.25 mg/kg/h), pancouronium (0.2 mg/kg/h) and ketamine (3 mg/kg/h). The animals were ventilated (“Julian”, Draeger, Vienna, Austria) with an FiO2 of 0.5, an I:E-ratio of 1:1.5, a positive end-expiratory pressure of 5 mmHg and a tidal volume of 10 ml/kg. The respiratory rate was adjusted continuously to maintain an end-tidal carbon dioxide partial pressure between 35 and 40 mmHg.

Sheaths were introduced into both carotid arteries and internal jugular veins. Under fluoroscopic guidance, a Swan-Ganz catheter (Edwards Lifesciences CCO connected to Vigilance I, Edwards Lifesciences, Irvine, CA, USA) was positioned in the left pulmonic artery, a quadripolar stimulation catheter in the high right atrium (Response 6F, St. Jude Medical, USA), a conductance catheter (5F, 12 electrodes, 7 mm spacing, MPVS Ultra, Millar Instruments, Houston, Texas, USA) in the left ventricle and a decapolar reference catheter (6F Dynamic Tip Steerable Catheter, Bard Electrophysiology, USA) was advanced into the coronary sinus. The body core temperature was measured at the tip of the Swan-Ganz-catheter. After instrumentation, a bolus of heparine (100 IE/kg) was administered, followed by a continuous infusion of 100IE/kg/h.

A balanced crystalloid infusion (Elo-Mel Isoton, Fresenius, Austria) was continuously administered at a fixed rate of 10 ml/kg/h. Urine outflow was enabled by a suprapubic catheter. After instrumentation, the animals were allowed to stabilize for 45 min.

2.1.3 Magnetic resonance imaging

Six DOCA pigs and a subgroup of 7 control pigs underwent magnetic resonance imaging using a 3T MR system (Magnetom Trio, Siemens Healthcare, Erlangen, Germany). Cardiac function was assessed from retrospectively ECG-gated, 2D segmented FLASH (fast low angle shot) cine images obtained under free breathing, using two-fold averaging to suppress breathing artefacts. For left ventricular (LV) function and muscle mass assessment the LV was covered by gapless slices in short axes orientation (measured temporal resolution 27ms interpolated to 40 cardiac phases per cardiac cycle; echo time, 2.7ms; flip angle 20degrees; voxel size, 1.9×1.6×8.0mm³), for atrial function evaluation, left and right atria were covered

by gapless slices in long axis orientation (measured temporal resolution 45ms interpolated to 25 cardiac phases per cardiac cycle; echo time, 2.9ms; flip angle 15 degrees; voxel size, 2.5×1.8×4.0mm³).

Left ventricular function parameters (end-diastolic volume, LVEDV; end-systolic volume, LVESV; ejection fraction, LVEF), left ventricular mass (LVMM; including papillary muscles and trabeculae to the myocardium) and atrial volumes were derived by manual segmentation (Figure 2) using the Simpson approach (Argus, Siemens, Erlangen, Germany). Left and right atrial maximum, minimum, and before contraction (Vbc) volumes as well as atrial total, passive and contractile EF were derived from respective volume vs. time curves (Figure 2).

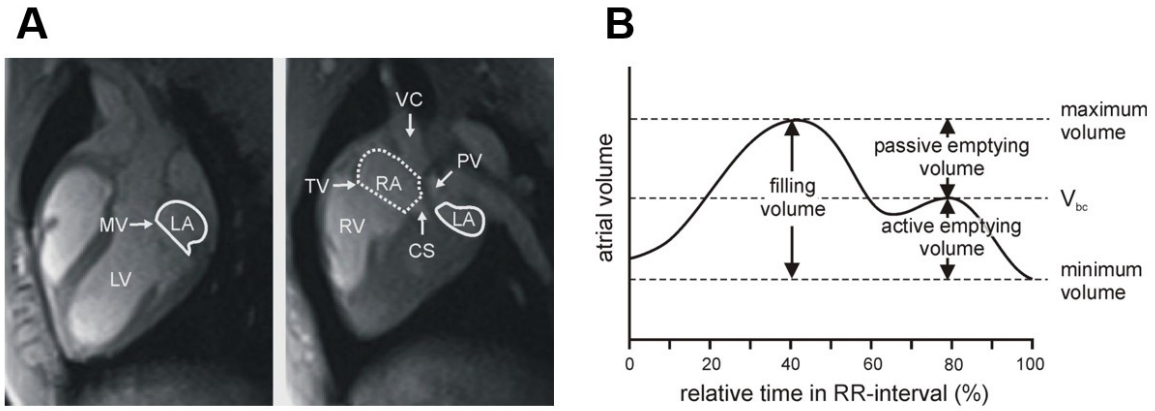

Figure 2. Volumetric measurements in MRI A: Representative MR images of left (LA) and right atrial (RA) segmentation. Left panel represents left atrium, mitral wave (MV) and left ventricle (LV). Right panel represents right and left atrium, vena cava superior (VC), pulmonary vein (PV), coronary sinus (CS), tricuspid valve (TV) and right ventricle (RV). B: Schematic atrial filling curve during one cardiac cycle representing filling volume (difference between maximum and minimum volume), passive emptying volume (difference between maximum volume and volume before contraction) and active emptying volume (difference between volume before contraction and minimum volume).

2.1.4 Electrophysiological study

After completion of MRI scans, animals were transferred to the electrophysiological lab. Atrial effective refractory period (AERP) was determined by an S1-S2 stimulation protocol (1 ms pulse at twice diastolic threshold at cycle lengths 400, 350 and 240 ms). AERP was determined using a train of 10 basic stimuli (S1) followed by a premature stimulus (S2) starting at S1-10 ms. S2 was delivered in decrements of 10 ms until capture was lost. The procedure was then repeated in 2 ms decrements within the final 10 ms window. AERP was defined as the longest S1-S2 interval failing to elicit a propagated response.

Inducibility of AF was assessed by burst protocols (1ms pulse at four times diastolic threshold, cycle lengths 200/150/100/50ms, 10s duration, 5 repetitions). An AF episode was defined as the onset of irregular atrial electrograms with an average cycle length shorter than 150ms for more than 10s.

2.2 Progression of atrial fibrillation in the presence of arterial hypertension

We previously established a porcine model of rapid atrial pacing (RAP)-induced AF.(218) In a first series, we could show that DOCA-induced arterial hypertension favours progression of the arrhythmia and increases mortality after 3 weeks of rapid atrial pacing. Here, we conducted a second series of animals focussing on the time point of two weeks rapid atrial pacing, to investigate structural and electrical remodelling that accounts for this faster disease progression.(1)

In short, healthy landrace pigs were implanted with pacemakers. After two weeks of recovery and would healing, DOCA pellets were implanted in a subgroup of animals. Two weeks later, rapid atrial pacing (RAP) was started and maintained for two weeks. Echocardiography and blood sampling were performed at baseline, at time of the pacemaker activation and prior to the sacrifice experiment. Regular rhythm checks were performed during pacemaker stimulation. Figure 3 shows a scheme of the experimental protocol.

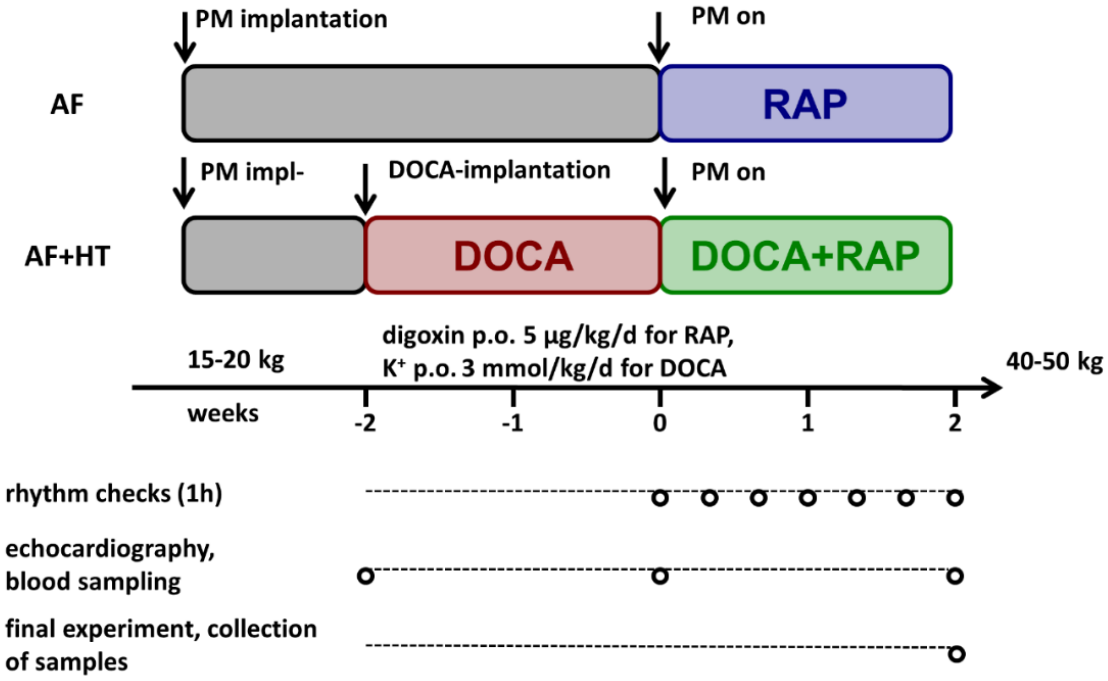

Figure 3. Scheme of the experimental protocol.

2.2.1 Pacemaker implantation

Telemetrically-controllable, custom made pacemakers and pacing probes were implanted in healthy landrace pigs under general anaesthesia.(1) Firstly, animals were sedated with an intramuscular injection of ketamine (20 mg/kg) and midazolam (0.5 mg/kg), followed by intravenous propofol (1 mg/kg) prior to orotracheal intubation. Anaesthesia was maintained with isoflurane (1-2%) and fentanyl (35 µg/kg/h). The respirator was set to an FiO2 of 50%, an I:E-ratio of 1:1.5, a positive end-expiratory pressure (PEEP) of 5 cm H_2O and a tidal volume of 10 ml/kg body weight. Respiratory rate was adjusted in order to keep the end-tidal carbon dioxide partial pressure between 35 and 40 mmHg. Median neck incision was performed, and the right internal jugular vein was prepared surgically. The jugular vein was incised and a pacemaker probe (Biotronik Setrox S45, Biotronik, Berlin, Germany) was implanted into the right atrial free wall under fluoroscopic guidance. A commercially available pacemaker (Evia, Biotronik, Berlin, Germany) and a programmer (ICS 3000, Biotronik, Berlin, Germany) were used to test sensing and pacing thresholds of the pacemaker probe. Proper lead positioning was controlled by fluoroscopy, the pacemaker was connected, proper connection was tested, and stimulation duration was set twofold the determined threshold. The pacemaker was then fixed in a surgically prepared pocket underneath the neck's musculature, and the neck was closed in layers using resorbable sutures. Surgical dressing was applied, anaesthesia was discontinued, and the animals were extubated.

The pigs recovered from the procedure for one week. During recovery, the animals received adequate pain medication (fentanyl transdermal system 100 µg/h, buprenorphine 10 µg/kg i.m.) and antibiotic treatment (penicillin/streptomycin i.m., amoxicillin/clavulanic acid p.o.). Oral administration of 5 µg/kg/d digoxin was started and maintained until the end of the protocol to slow atrio-ventricular conduction. Digoxin levels were measured in plasma samples repetitively and the dose was adjusted to maintain plasma levels of 1.0-2.0 µg/l (clinical therapeutic range: 0.5-2.0 µg/L).

2.2.2 DOCA implantation

After at least one week of wound healing, a subgroup of animals (AF+HT) underwent implantation of DOCA-pellets (100mg/kg, 60-day release pellets, Innovative Research of America, Sarasota, FL, USA) subcutaneously into the inguinal region under sedoanalgesia (20 mg/kg ketamine, 0.4 mg/kg midazolam, 0.5 mg/kg azaperone) and a sugar-, salt- and potassium-rich diet was subsequently started.(1)

After two weeks, right atrial pacing at a rate of 600/min was started in both AF and AF+HT groups.

2.2.3 Echocardiography

At baseline (PM activation) and two weeks after onset of RAP, animals were sedated and transthoracic echocardiography (Vivid I, GE Healthcare, Vienna, Austria) was performed to record parasternal short- and long-axis 2D-views. During the measurements, RAP was interrupted transiently. Left ventricular (LV) dimension and wall thicknesses were obtained in short and long-axis views, left atrial (LA) area was obtained from the long-axis view. Data were analysed off-line and averaged over three subsequent beats by a blinded investigator.(1)

2.2.4 Final experiment

The experimental setup has been described before.(1, 218) Animals were fasted overnight with free access to water and sedated with 0.5 mg/kg midazolam and 20 mg/kg ketamine. After administration of 1 mg/kg propofol, orotracheal intubation was performed and anaesthesia was maintained with sevoflurane (1%), fentanyl (35 µg/kg/h), midazolam (1.25 mg/kg/h), pancouronium (0.2 mg/kg/h) and ketamine (3 mg/kg/h). The animals were mechanically ventilated (ventilator: “Julian”, Draeger, Vienna, Austria) with an FiO2 of 0.5, an I:E-ratio of 1:1.5, a positive end-expiratory pressure of 5 mmHg and a tidal volume of 10 ml/kg. The respiratory rate was

adjusted to maintain an end-tidal carbon dioxide partial pressure between 35 and 40 mmHg.

After initial stabilisation, surgical preparation of the neck was performed, sheaths were introduced into both carotid arteries and internal jugular veins. Under fluoroscopic guidance, a quadripolar stimulation catheter was positioned in the high right atrium (Response 6F, St. Jude Medical, USA), a conductance catheter (5F, 12 electrodes, 7 mm spacing, MPVS Ultra, Millar Instruments, Houston, Texas, USA) in the left ventricle, a Swan-Ganz catheter (Edwards Lifesciences CCO connected to Vigilance I, Edwards Lifesciences, Irvine, CA, USA) in the left pulmonic artery and a decapolar reference catheter (6F Dynamic Tip Steerable Catheter, Bard Electrophysiology, Lowell, MA, USA) was advanced into the coronary sinus. Body core temperature was measured at the tip of the Swan-Ganz-catheter.

Surgical preparation of both groins was performed, an arterial line was introduced into the right femoral artery to invasively monitor arterial pressure. Sheaths (14F) were introduced into both femoral veins, and a steerable sheath (Agilis, St. Jude Medical, Lowell, MN, USA) with a quadripolar 4 mm tip mapping catheter (Thermocool, Biosense Webster, Johnson & Johnson, Irvine, CA, USA) as well as a monophasic action potential (MAP) catheter (6F, four-electrode tip, two reference electrodes, Medtronic, Minneapolis, MN, USA) were positioned under fluoroscopic guidance first in the right atrium and subsequently in the left atrium after transseptal puncture using the mapping catheter.

After instrumentation, a bolus of heparin (100 IE/kg) was administered, followed by a continuous infusion of 100IE/kg/h.

A balanced crystalloid infusion (Elo-Mel Isoton, Fresenius, Vienna, Austria) was continuously administered at a rate of 10 ml/kg/h. Suprapubic catheterisation was performed to enable urine outflow. After instrumentation, the animals stabilized for 45 min.

2.2.5 Electrophysiological study

RAP was interrupted at the beginning of the sacrifice experiment and AF duration was measured until spontaneous conversion to sinus rhythm occurred.(1)

Atrial effective refractory period (AERP) was determined by an S1-S2 stimulation protocol (1 ms pulse at twice diastolic threshold at cycle lengths 400, 350, 300, 250 and 200 ms). AERP was determined using a train of 10 basic stimuli (S1) followed by one premature stimulus (S2) starting at S1-10 ms. The premature stimulus was delivered in decrements of 10 ms until capture was lost. The procedure was repeated in 2 ms decrements within the final 10 ms window. AERP was defined as the longest S1-S2 interval failing to elicit a propagated response.

The MAP catheter was positioned on the right and left atrial free walls. Pacing at different cycle lengths (400, 350, 300, 250 and 200 ms) was performed from the high right atrium for RA measurements and from the coronary sinus for LA measurements to assess action potential duration (APD). APD was measured using a custom-made software (Matlab, Mathworks Inc., Natick, MA, USA) and verified manually. The action potential (AP) upstroke was set to the calculated maximal dV/dt after the pacing stimulus. Phase 2 was defined immediately after the AP peak. Phase 4 diastolic voltage was set manually in case a pacing artefact was present in this area. An APD at 90% repolarization (APD90) extended from AP onset to 90% voltage recovery from phase 2. The diastolic interval extended from APD90 of the prior beat to the current AP onset.(94, 223)

2.2.6 Endocardial mapping

Maps of both atria were constructed using the electroanatomical mapping system CARTO™ XP (Biosense Webster, Johnson & Johnson, Irvine, CA, USA).(1) The mapping system's technology has been described in detail previously.(224) In brief, the system records surface electrocardiograms (ECGs) and bipolar electrograms filtered at 30 to 400 Hz from the mapping catheter and reference catheters (in our case: coronary sinus catheter). Points were manually acquired, when catheter as

wells as electrogram stability were given. Points were equally distributed, and a fill-threshold of 15 mm was used. Points were edited offline. Local activation time (in reference to the coronary sinus catheter) was manually annotated to the peak of the largest amplitude deflection on the bipolar electrograms. The earliest potential was annotated in case of double potentials.

A three-dimensional atrial surface model was built using Matlab (R2013b, Mathworks Inc., Natick, MA, USA) to automatize conduction velocity measurements within the mesh constructed by CARTO™ (Figure 4). Conduction velocities during S1 pacing were calculated using an automated method based on the approach by Bayly et al.(225)

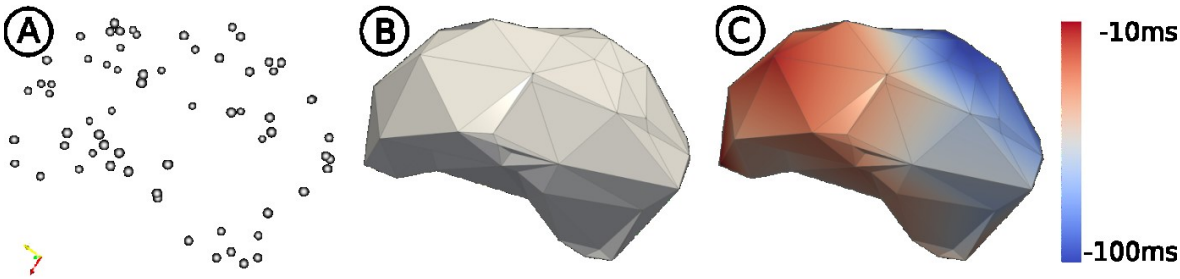

Figure 4. Construction of endocardial maps. A) Point cloud of data acquisition sites used during mapping procedure in 3D space. B) Triangulated atrial surface geometry in 3D reconstructed from point cloud with interpolated referenced local activation times shown in (C) (colour coded from red (earliest activation) to blue (latest activation)).(1)

2.2.7 Epicardial multielectrode mapping

Median thoracotomy was performed after endocardial mapping to allow contact mapping of the atria.(1) The pericardium was opened for 2-3 cm to place a custom-made, squared high-density mapping electrode array (16x16 channels, 1.5 mm interelectrode distance) on the right and subsequently on the left atrial free wall. To measure conduction velocities, pacing at cycle lengths of 500, 450, 400, 350, 300 and 250 ms was performed either at the high right atrium (RA measurements) or the

proximal coronary sinus (LA measurements). AF was then re-induced by burst stimulation and fibrillation electrograms were recorded for 30s (sampling rate 1 kHz, filtering bandwidth 0.5-500 Hz).

A probabilistic electrogram algorithm was used to identify local deflections in each recorded electrogram. Individual fibrillation waves were delineated by boundaries of conduction block. Conduction block was assumed if local conduction velocity was lower than 20 cm/s. Depending on their origin within the array, waves were classified as peripheral waves or epicardial breakthroughs. For each activation at each electrode, a plane was fitted to activation times at neighbouring electrodes belonging to the same wave. The plane indicates conduction velocity and local direction of propagation.(88, 89) Complexity parameters such as waves per cycle length, wave size, conduction velocity, maximum dissociation and fractionation as well as AF cycle length were analysed using custom-made Matlab-based software.(226)

In short, activation time points on the multielectrode array were grouped into separate fibrillation waves. Size of these waves as well as the number of waves present on the array within the AF cycle length were quantified. Fractionation of signals represents activation of surrounding waves picked up by the mapping electrode, thus showing a more complex fibrillatory pattern. Increased interstitial fibrosis potentially leads to electrical dissociation within the epicardial layer by uncoupling side-to-side connections between muscle bundles, which can also be quantified using the multielectrode array.(88, 89)

2.2.8 Blood samples

At each step of the experimental protocol, arterial blood samples were processed immediately after withdrawal. A blood gas analyser (ABL 600; Radiometer, Copenhagen, Denmark) was used for the temperature-corrected measurements of oxygen saturation, partial oxygen pressures, carbon dioxide pressures, pH, acid-base status, haemoglobin, lactate and electrolytes.(1)

2.2.9 Tissue samples

After epicardial mapping was completed, ascending aorta, pulmonary artery and venae cavae were clamped and a cardioplegic solution (100 mmol of potassium chloride) was injected into the ascending aorta proximally of the clamp.(1) The heart was explanted, rinsed carefully using saline and both atria were dissected. The right atrium was cut along the interatrial septum, the tricuspid annulus and junctions of superior and inferior caval veins. The left atrium was cut along the interatrial septum, the mitral annulus, and the common ostium of the pulmonary veins. Atria were then weighed using a gram scale (Kompakt EMB 600-2, Kern & Sohn GmbH, Balingen, Germany) and stored in 4% paraformaldehyde in phosphate buffer solution for further histological sampling.

2.2.10 Tissue processing

Transmural tissue blocks of left atria were fixed in 1.5% glutaraldehyde and 1.5% paraformaldehyde in 0.15M Hepes buffer and cut according to the systematic uniform random sampling procedure.(1) In short, 1/k slices are to be sampled, a random number between 1 and k is chosen using a random number table, and starting from that slice, every kth slice is sampled.(227)

2.2.10.1 Paraffin

For quantification of fibrosis, specimens were embedded in paraffin, 3 µm sections were cut and stained with Picrosirius red.(228) Representative images at an objective lens magnification of 10x were prepared using an Axio Scan Z1 slide scanner (Zeiss, Oberkochen, Germany) and analysed using Adobe Photoshop CS6 (version 13.0 x32). For each tissue slice, fibrosis was measured as the percentage of total tissue area stained by picrosirius red per microscopic field.

2.2.10.2 Epoxy resin

For quantification of cardiomyocyte organelles volumes and collagen volumes, samples were postfixed in 1% osmium tetroxide solution, stained in half-saturated uranyl acetate solution and embedded in epoxy.(228) Sections of 1 µm thickness were stained with toluidine blue and imaged with a Leica DM6000B microscope (Leica, Wetzlar, Germany) at an objective lens magnification of 40x (Zeiss, Oberkochen, Germany) for stereological light microscopy (LM) analysis. Sections of 60 nm thickness were stained with uranyl acetate/lead citrate and imaged with a transmission electron microscope (Morgagni; FEI, Eindhoven, the Netherlands) at a primary magnification of 8,900x for stereological electron microscopy (EM) analysis.(229)

2.2.10.3 Design-based stereology

Six animals per group were included for design-based stereological analysis. Left atrial volumes were calculated by division of atrial weight by the density of muscle tissue (1.06 g/cm^3).(230) Fields of view were obtained by systematic uniform random sampling (method: see above), the newCAST stereology software was used in case of LM analysis (Visiopharm, Horsholm, Denmark).(231) Volume estimation was performed using the point-counting method.(227, 232) Volumes of cardiomyocyte organelles and collagen were obtained using EM, volumes of cardiomyocytes and interstitium were estimated using LM. Mitochondria, myofibrils, nuclei and sarcoplasm were differentiated within cardiomyocytes. Interstitial collagen was subdivided according to its localization 1) in between cardiomyocytes or 2) at other localizations including perivascular collagen.

2.2.10.4 Immunohistochemistry

For staining of connexin 43, slides were deparaffinised, blocked with 1% BSA, incubated with the primary antibody (Abcam ab11370) and the secondary antibody

(Alexa Fluor 488 goat anti rabbit IgG, Invitrogen, A11034). Cell membranes were stained with WGA (wheat germ agglutinin, Alexa Fluor 555 conjugate, Invitrogen, W32464) and nuclei were stained with DAPI (4',6-diamidino-2-phenylindole).

Slides were placed on the stage of an inverted microscope equipped with a Plan Neofluar 40x/1.3 N.A. oil-immersion objective and a Zeiss LSM 510 Meta confocal laser point scanning system (Zeiss, Jena, Germany). Excitation and emission wavelengths were 488/518nm for Alexa Fluor, 555/568nm for WGA and 358/460nm for DAPI, respectively. The pinhole was set to 1 Airy unit, resulting in an optical slice thickness of 0.9µm. The confocal plane (z-axis) was set to the equatorial plane of the cardiomyocyte. Distribution of connexin 43 was measured by calculation of the ratio of intensity of connexin 43-positive staining along the lateral sides and intercalated discs of the cardiomyocytes.

2.2.11 Computer Modelling

In order to mechanistically link electrical and structural remodelling with AF stability, computational modelling was performed.(1) Using mean APD90 and AERP from in vivo experiments as well as atrial dimensions measured with echocardiography from the in vivo model, a three-dimensional atrial shell model was developed, and re-entrant activity was induced using a S1-S2 protocol to test for arrythmia stability (Figure 5).

The *in silico* atrial model was based on a monodomain description of cardiac tissue given as

$$\beta C_m \frac{\partial V_m}{\partial t} = \nabla \cdot \boldsymbol{\sigma}_m \nabla V_m - \beta I_{ion}(V_m, \eta),$$

where β is the bidomain surface-to-volume ratio, C_m is the membrane capacitance, $\boldsymbol{\sigma}_m$ is the harmonic mean conductivity tensor, $V_m = \phi_i - \phi_e$ is the transmembrane voltage and I_{ion} are ionic currents depending on and the state variables, η, governed by

$$\frac{\partial \boldsymbol{\eta}}{\partial t} = f(\boldsymbol{\eta}, t).$$

In absence of data on fibre architecture tissue was assumed to be isotropic, that is, $\boldsymbol{\sigma}_m \coloneqq g_m \cdot \boldsymbol{I}$.

In absence of detailed tomographic data on atrial anatomy ultrasound-based measurements of the long parasternal axis, L, and the shorter transverse axis, R, were used to build an ellipsoidal thin-walled shell model that approximates the true anatomy of the LA. The axes of the ellipsoids were chosen as $L = 35.9/42.3$ mm and $R = 32.3/41.6$ mm for the AF and AF+HT models, respectively. These dimensions were based on the average of all $n = 17$ echocardiographic measurements. Discrete ellipsoidal geometry models consisting of triangular elements were generated using Gmsh with an average spatial resolution of $dx \approx 237$ µm.(233) The electrophysiology model was parameterized to match the wavelength, λ, observed experimentally, that is, $\lambda = \text{ERP} \times v \approx APD_{90} \times v$, where ERP is the effective refractory period, APD_{90} is the action potential duration until 90% repolarization, and v is the average conduction velocity. In single cell pacing experiments, the ionic model was set up to approximate the APD_{90}=120 ms observed in both AF and AF+HT experiments. We refrained from using a more detailed atrial action potential model for various reasons. First, the main parameter of interest was APD_{90} which can be represented in any ionic model, and, secondly, porcine-specific atrial models of cellular dynamics are not available. We have chosen therefore the simple modified Beeler-Reuter-Drouhard-Roberge model as APD_{90} is readily adjustable to a wide range of action potential durations. (234, 235) Parameters affecting conduction velocity such as β, upstroke velocity of a given action potential as well as intra- and extracellular conductivities were estimated in an automated iterative tuning procedure.(236) The parameters which led to the sought-after velocity of 1.2 m/s for the given spatial resolution were found as $g_m = 0.42$ Sm^{-1} and $\beta = 1400\ cm^{-1}$.

The exact same parameters and protocols were applied to both the AF and AF+HT models with the only difference being between ellipsoidal geometry of the models which was marginally larger in the AF+HT model. Reentrant activation was induced using a S1-S2 stimulus protocol. A single $S1$ transmembrane current stimulus was delivered at the $-z$ pole of the ellipsoid to initiate propagation. $S2$ was delivered then to the lower left shell of the ellipsoid (seen in the yz-plane) and also to the upper posterior section (see Figure 5). With the given APD_{90} were vulnerable to induction

within a coupling interval CI ranging from 110 ms to 150 ms. With these settings a phase singularity was created at the intersection of the critical recovery isoline with the edges of the S2 stimulus and left the upper anterior shell as the main pathway for the induced rotor to move. The vulnerable window was sampled at a temporal resolution of $\Delta CI = 0.5$ ms, resulting in a total of 80 different reentrant activation patterns, that is, 40 for AF and AF+HT, respectively. In all simulations, reentrant activity was monitored for up to 10 s. If activity was still present after 10 s the arrhythmia was deemed sustained.

The propensity towards reentrant patterns was assessed by measuring the number of episodes lasting for at least $\geq 1\ s$, $N_{>1s}$, and among these the average duration, $\bar{F}_{>1s}$, was determined. In all simulations for each coupling interval CI the duration of each reentrant episode was recorded.

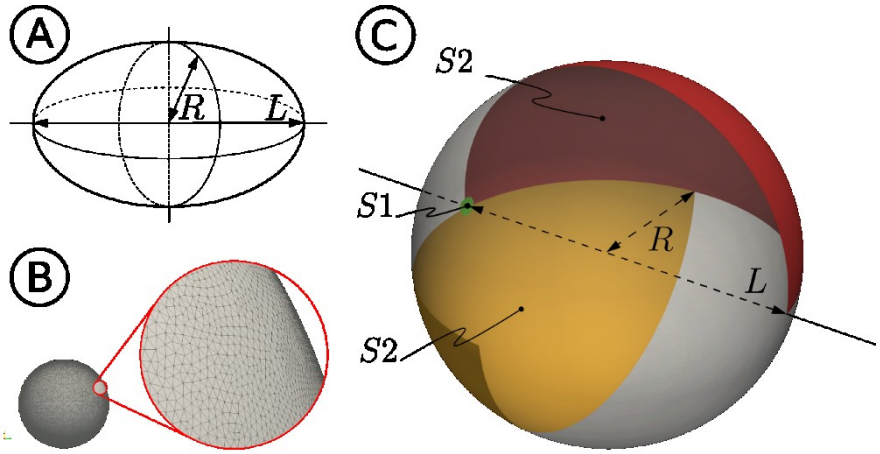

Figure 5. Three-dimensional computational model. A) Approximation of an atrial anatomy as an ellipsoid defined by R and L. B) Anatomical meshes of the atria using an average spatial resolution of dx=237μm. C) Electrode patches used in the S1-S2 protocol.(1)

2.3 Statistics

Continuous variables are presented as mean±SD or median (interquartile range). Categorical variables are presented as percentages and counts.

Two-group comparisons of normally distributed continuous variables were performed by Student's t tests. If the normality assumption was violated according to Shapiro-Wilk tests or visual inspection of normal probability plots, two-group comparisons were performed by Wilcoxon rank-sum tests.

Categorical variables were compared using chi-squared tests. Repeated electrophysiological measurements at different cycle lengths and pacing steps were compared by 2-way repeated measurement analysis of variance (ANOVA). Tukey's test was used for post-hoc analysis.

Two-tailed P values <0.05 were considered to indicate statistical significance. Graphs were plotted with Prism 6 (GraphPad Software Inc., La Jolla, CA, USA), statistical analyses were performed with SPSS 23.0 (IBM, Armonk, NY, USA).(1)

3 Results

For the first series, 15 animals were implanted with DOCA pellets, while 23 animals served as controls. Electrophysiological studies were performed in 7 DOCA animals and 8 controls, MRI war performed in 6 DOCA animals and 7 controls, histological analysis was performed in 8 DOCA animals and 8 controls.

For the second series, 18 animals were implanted with DOCA pellets, a subgroup of 10 animals were implanted with pacemakers. One animal in the AF group was excluded due to PM lead dislocation. Data from echocardiography and the final experiment were complete for 9 animals in the AF+HT and 8 animals in the HT group. Six animals from each group were included in the stereological analysis.(1)

3.1 Development of atrial fibrillation in the presence of arterial hypertension

Twelve weeks of DOCA treatment lead to a significantly increase in arterial blood pressure (systolic blood pressure measured with tail cuff: 142±37 mmHg in DOCA vs. 97±6 mmHg in controls, $p<0.05$), an increased left ventricular myocardial mass (134±21 mmHg in DOCA vs. 100±19 mmHg in controls), while left ventricular ejection fraction measures with echocardiography remained unchanged (53± 4% in DOCA vs. 52±3% in controls; Figure 6).

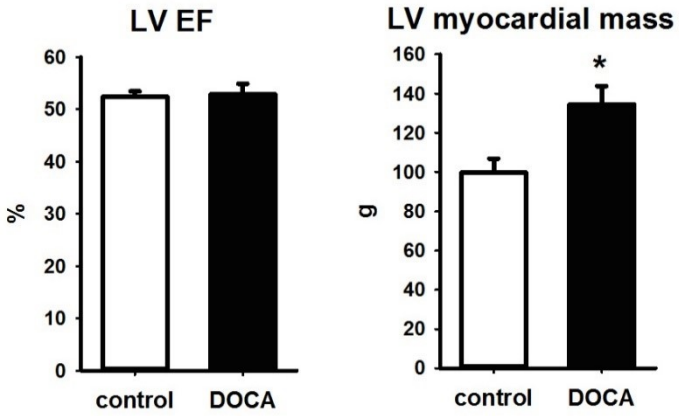

Figure 6. LV function and mass. Left panel: Left ventricular ejection fraction (EF) was within a normal range and comparable between both groups (p=n.s.). Right panel: Myocardial mass (g) was significantly larger in animals subjected to DOCA. Asterisks indicate p<0.05, whiskers indicate SEM.

Both left and right atrium showed no increase in collagen content (LA: 6.7±1% in DOCA vs. 5.3±3% in controls; RA: 5.4±2% vs. 7.8±4%; each n.s.; see Figure 7 and Figure 8) but extensive cardiomyocyte hypertrophy (LA: 171.8±15 μm^2 vs. 114.5±25 μm^2; RA: 330.1±115 μm^2 vs. 172.4±40 μm^2; each p<0.05; see Figure 9).

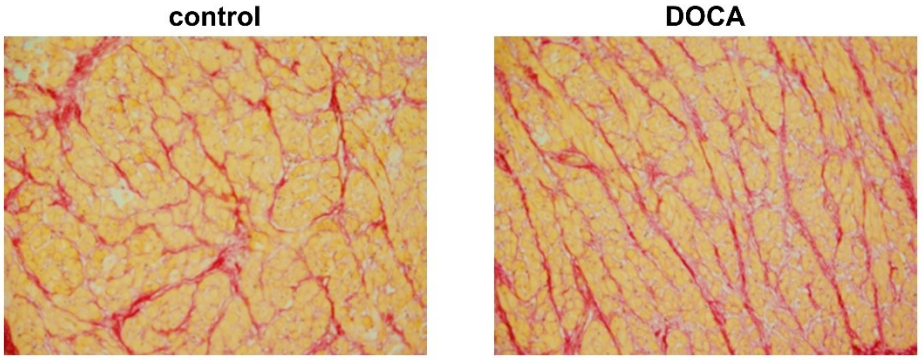

Figure 7. Atrial collagen distribution. *Representative picro-sirius-red stainings of samples of animals for DOCA and control group.*

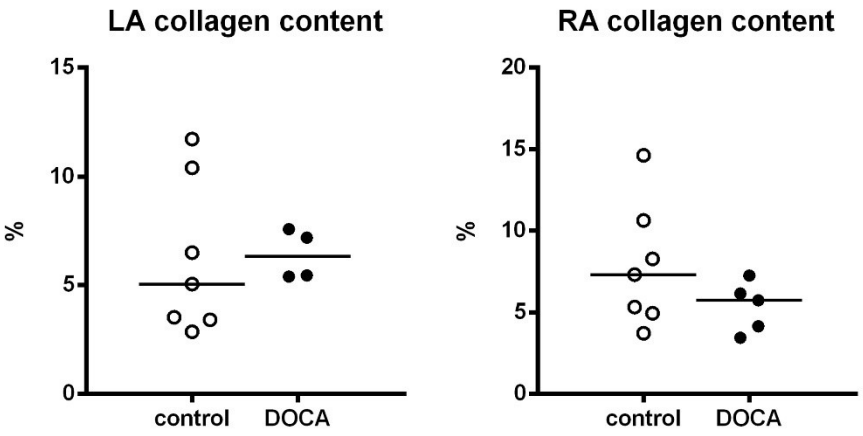

Figure 8. Left and right atrial collagen content. *There was no difference in left and right atrial collagen content between animals subjected to DOCA and controls.*

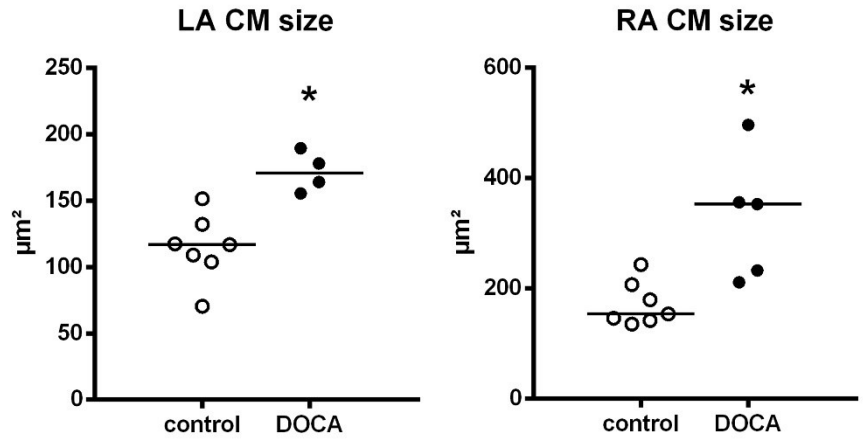

Figure 9. Left and right atrial cardiomyocyte (CM) size. *Cardiomyocytes show a significantly larger area in both atria of DOCA-pigs as compared to controls in HE stained histologic samples. Asterisks indicate p<0.05.*

For functional assessment, in vivo left and right atrial function were studied. Left atrial end-diastolic (Vmax) and end-systolic volumes (Vmin) as well as volume before contraction (Vbc, see Figure 10) were increased in DOCA-treated animals (Figure 10). This resulted in an impaired total left atrial ejection fraction (contractile + passive ejection fraction) as well as contractile ejection fraction in the DOCA group. In the right atrium, end-diastolic volume (Vmax, see Figure 10) was increased

and there was a trend towards similar changes in total and contractile ejection fraction as in the left atrium (Figure 10).

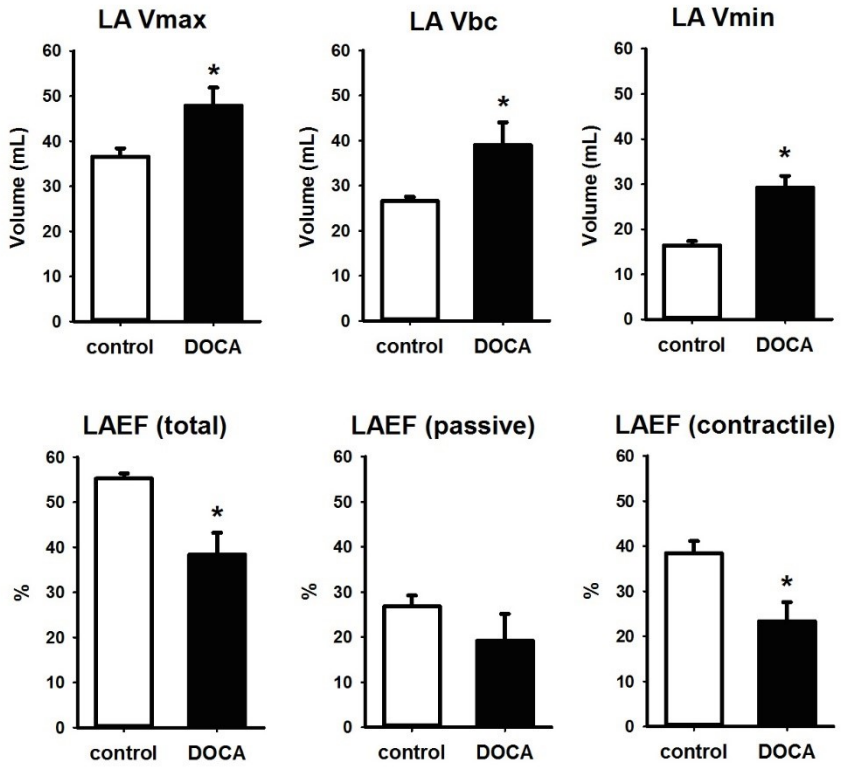

Figure 10. Left atrial volumetric data from MRI study. Top left panel: Left atrial maximum volume (LA Vmax) was significantly higher in animals subjected to DOCA as compared to controls. Top centre panel: Left atrial volume before contraction (LA Vbc) was significantly higher in DOCA animals. Top right panel: Left atrial minimal volume (LA Vmin) was significantly higher in DOCA animals. Bottom right panel: Left atrial total ejection fraction (EF) was significantly lower in DOCA animals. Bottom centre panel: Left atrial passive ejection fraction was comparable between both groups. Bottom right panel: Left atrial contractile ejection fraction was significantly lower in DOCA animals. Asterisks indicate p<0.05, error bars indicate SEM.

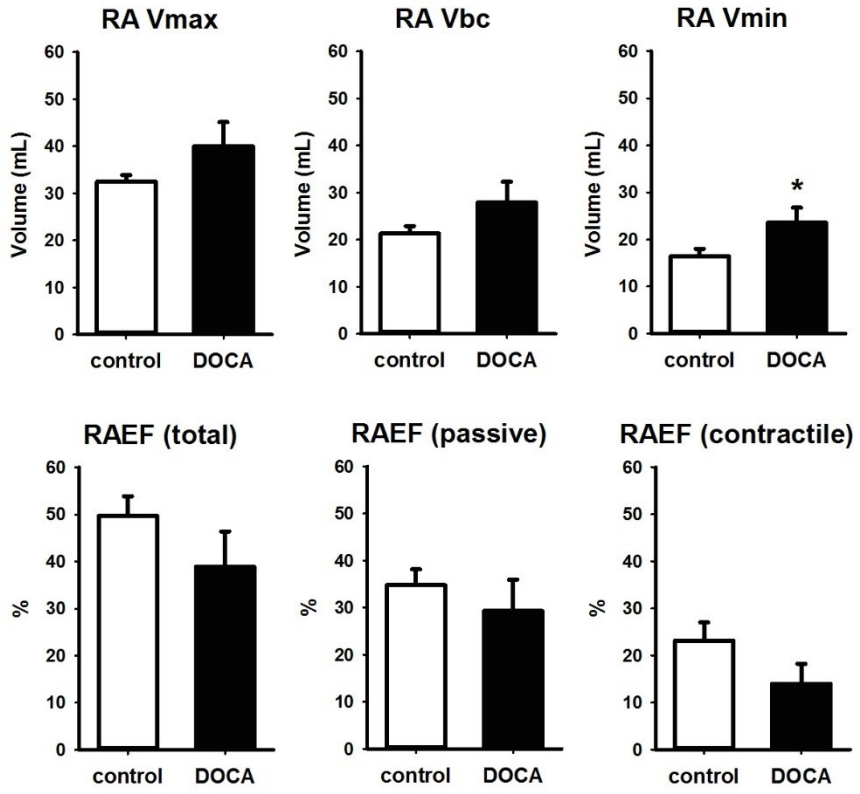

Figure 11. Right atrial volumetric data from MRI study. Top left panel: Right atrial maximum volume (RA Vmax) was significantly higher in animals subjected to DOCA as compared to controls. Top centre panel: Right atrial volume before contraction (RA Vbc) was significantly higher in DOCA animals. Top right panel: Right atrial minimal volume (RA Vmin) was significantly higher in DOCA animals. Bottom right panel: Right atrial total ejection fraction (EF) was significantly lower in DOCA animals. Bottom centre panel: Right atrial passive ejection fraction was comparable between both groups. Bottom right panel: Right atrial contractile ejection fraction was significantly lower in DOCA animals. Asterisks indicate p<0.05, whiskers indicate SEM.

AF inducibility (episodes >10s) was significantly higher in DOCA-treated animals (74±28% of all stimulations in DOCA vs. 40±30% in controls; p<0.05; see Figure 12). AF duration was unaltered (17±2s in DOCA vs. 12±7s in controls, p=n.s.). AERP showed no differences (S1=400ms: 187±37ms in DOCA vs. 185±27ms in control; S1=300ms: 164±26ms vs. 179±30ms; S1=240ms: 163±44ms vs. 179±26ms; p=n.s., Figure 13). Serum potassium levels during the stimulation

protocol were comparable in both groups (4.1±0.2 in DOCA vs. 4.1±0.4 in controls, p=n.s.).

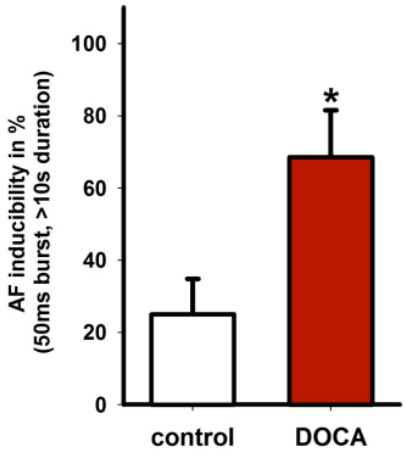

Figure 12. AF inducibility in DOCA vs. control. After 50 ms burst stimulation, AF episodes lasting longer than 10 seconds were more frequent in animals subjected to DOCA (red column) compared to controls (white column). Asterisks indicate p<0.05, whiskers indicate SEM.

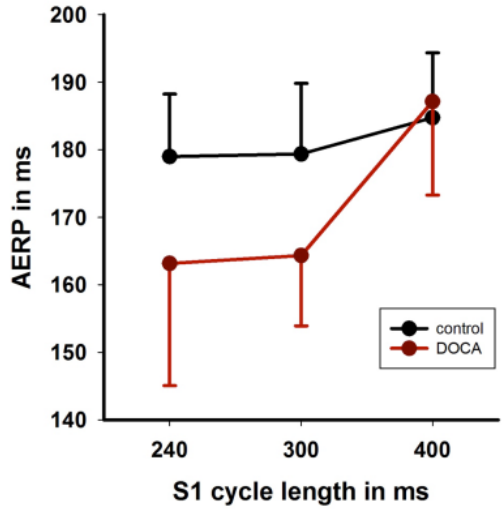

Figure 13. Atrial effective refractory periods (AERP) in DOCA vs. control. Right AERP did not differ between animals subjected to DOCA (red) and controls (black) at S1 pacing cycle lengths 240, 300 and 400ms. Whiskers indicate standard deviation.

3.2 Progression of atrial fibrillation in the presence of arterial hypertension

One animal in the AF group was excluded due to dislocation of the PM lead into the right ventricle. Both groups had comparable body weights (AF+HT: 46.3±6.1 kg, AF: 44.9±4.5 kg, p=0.6) at the time of the final experiment. After pacemaker deactivation, more animals in the AF+HT group (5/9) than in the AF group (1/8) were in AF for longer than one hour (p<0.001, Figure 14). Median AF duration after PM deactivation was longer in the AF+HT group (76.7 (0-210) min) than in the AF group (18.8 (0-150) min, p=0.025).(1)

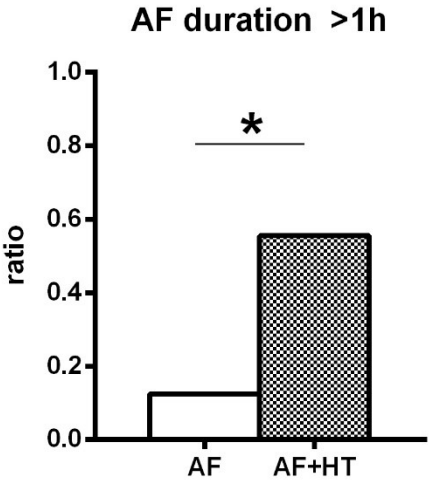

Figure 14. AF duration. Significantly more animals in the AF+HT group had AF episodes lasting longer than 1h (p<0.05). This figure contains data from Manninger M et al., Heart Rhythm. 2018 Sep;15(9):1328-1336.(1)

3.2.1 Echocardiography

Echocardiography revealed increased left atrial cross-sectional areas (LA dilatation) in the AF+HT group compared to the AF group, both at the time point of PM activation (1 week of DOCA administration) and at the final experiment. LA cross-

sectional area at the terminal experiment was 11.9±3.1 cm² in the AF+HT group and 7.8±2.3 cm² in the AF group (p=0.008, Figure 15). AF+HT animals showed concentric left ventricular hypertrophy (relative wall thickness 0.52±0.02 in the AF+HT group and 0.38±0.01 in the AF group; p=0.0002, Figure 16).(1)

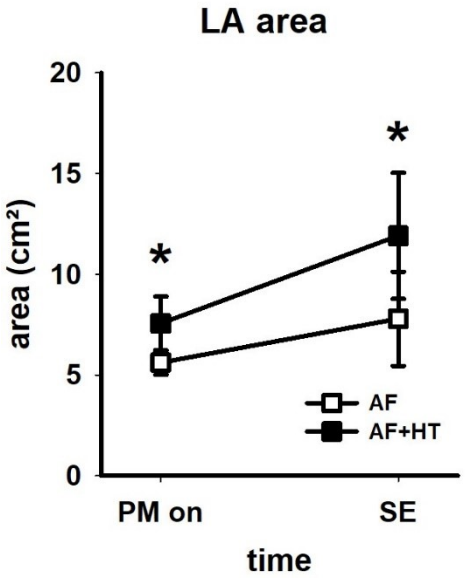

Figure 15. Left atrial (LA) area over time. LA area measured by echocardiography at the time point of pacemaker activation (PM on) and the sacrifice experiment (SE, two weeks later). Cross-sectional left atrial area was larger in the AF+HT group than in the AF group both at PM activation and at the time of the sacrifice experiment (p<0.05). This figure contains data from Manninger M et al., Heart Rhythm. 2018 Sep;15(9):1328-1336.(1)

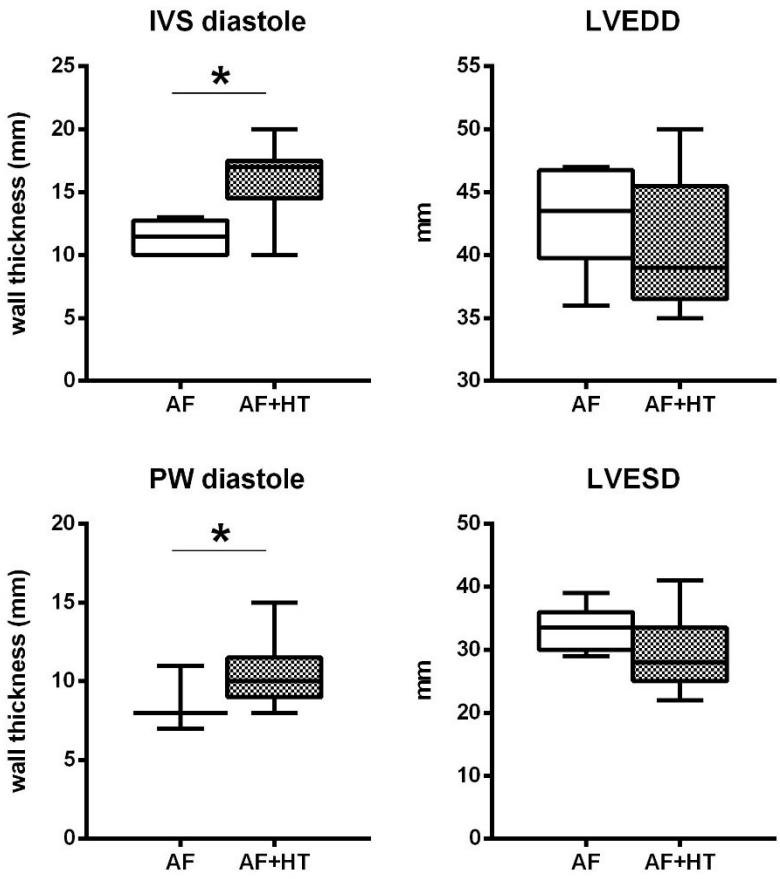

Figure 16. Left ventricular structural changes in echocardiography. At the time of the sacrifice experiment, animals in AF+HT showed no left ventricular dilatation (no difference in left ventricular end-diastolic (LVEDD) and end-systolic (LVESD) diameter), but increased wall thicknesses ($p<0.05$) of the intraventricular septum (IVS) and posterior wall (PW) during diastole. This figure contains data from Manninger M et al., Heart Rhythm. 2018 Sep;15(9):1328-1336.(1)

3.2.2 Hemodynamics

Animals in the AF+HT group showed significantly higher mean aortic pressures than in the AF group (Table 1).(1)

At the beginning of the sacrifice experiment, the pacemaker was deactivated and time until conversion into sinus rhythm was measured as mentioned above. After conversion to sinus rhythm, both groups showed comparable heart rate, pulmonary arterial pressure (PAP), cardiac output (CO), central venous pressure (CVP), left

ventricular end diastolic pressure, maximum dP/dt (change of pressure over time) and left atrial pressure.(1)

	AF	AF+HT	p
n	8	9	
weight (kg)	44.9±4.5	46.3±6.1	0.602
mean AOP (start, mmHg)	82.8 (79;96)	109.9 (100;137)	0.018
heart rate (bpm)	101.6 (89;105)	111.8 (97;116)	0.136
CO (L/min)	4.6±1.2	4.6±0.8	0.900
mean PAP (mmHg)	24.5 (21;26)	21.6 (16;27)	0.597
mean CVP (mmHg)	5.0±1.2	3.6±2.0	0.100
LVEDP (mmHg)	13.1±5.4	11.6±4.8	0.599
dP/dt max (µg/kg/min)	1.85 (1.64;3.45)	1.98 (1.62;2.12)	0.779
mean LA pressure (mmHg)	7.6±2.6	9.6±4.6	0.324

Table 1. Hemodynamic parameters during the final experiment in general anesthesia. Animal in the AF+HT group had higher mean aortic pressure (AOP) as compared to animals in the AF group. There were no differences in cardiac output (CO), pulmonary arterial pressure (PAP), central venous pressure (CVP), left ventricular end diastolic pressure (LVEDP), maximum dP/dt (change of pressure over time) or mean left atrial (LA) pressure. This table contains data from Manninger M et al., Heart Rhythm. 2018 Sep;15(9):1328-1336.(1)

3.2.3 Structural remodelling

Both left and right atrial tissue weights were significantly higher in the AF+HT group than in the AF group (Figure 17). Atrial tissue weights in the AF+HT group remained significantly higher, also after correction for body weight. LA weights corrected for body weight were 0.727±0.06 g/kg in the AF+HT group and 0.559±0.05 g/kg in the AF group (p=0.049). RA weights corrected for body weight were 0.515±0.02 g/kg in the AF+HT group and 0.432±0.02 g/kg in the AF group (p=0.007).(1)

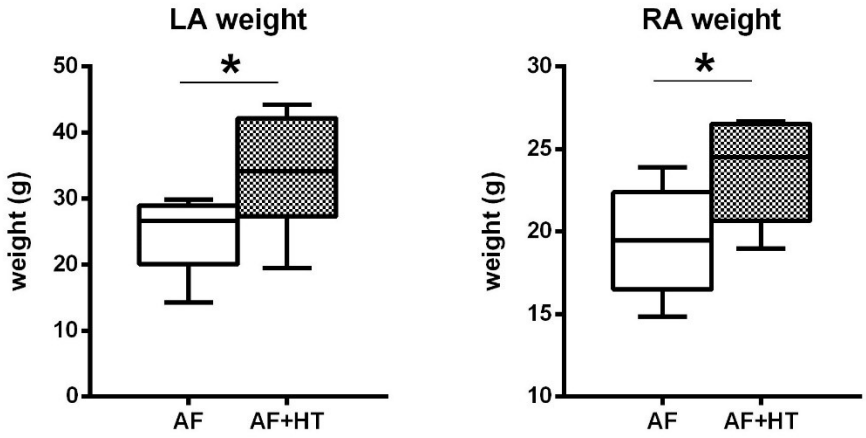

Figure 17. Atrial weights. Weights of dissected left (LA) and right (RA) atrial were significantly higher in the AF+HT group compared to the AF group (p<0.05). This figure contains data from Manninger M et al., Heart Rhythm. 2018 Sep;15(9):1328-1336.(1)

Stereological analysis of the left atrium revealed increased total collagen volume (1.95±0.45 cm³ in AF+HT vs. 1.18±0.34 cm³ in AF; p=0.0087, Figure 18, Figure 19). Intermyocyte collagen volume was comparable between both groups (0.33±0.13 cm³ in AF+HT vs. 0.22±0.07 cm³ in AF; p=0.093), while in AF+HT, volume of non-intermyocyte collagen (collagen at perivascular regions and between cardiomyocyte bundles) was significantly increased (1.62±0.38 cm³ in AF+HT vs. 0.96±0.31 cm³ in AF; p=0.0087). Total myofibril and myocyte volumes were comparable between both groups (Figure 20).(1)

There were no significant differences in sarcoplasmic (7.34±2.9 cm³ in AF+HT vs. 6.99±2.7 cm³ in AF; p=0.830), mitochondrial (2.78±1.2 cm³ in AF+HT vs. 1.80±0.4 cm³ in AF; p=0.095) and nucleic (0.31±0.1 cm³ in AF+HT vs. 0.30±0.1 cm³ in AF; p=0.853) volumes between both groups.(1)

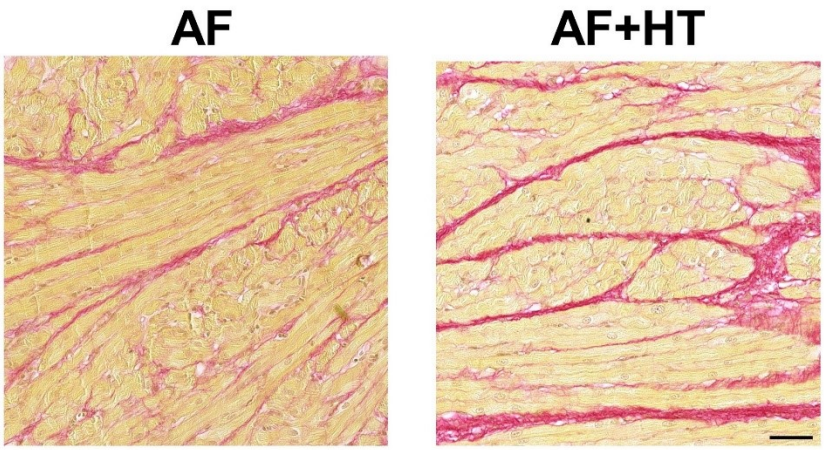

Figure 18. Atrial collagen content - sample images. Histological samples of animals for the atrial fibrillation (AF) group and AF + arterial hypertension (HT) group stained with picro-sirius-red. This figure contains data from Manninger M et al., Heart Rhythm. 2018 Sep;15(9):1328-1336.(1)

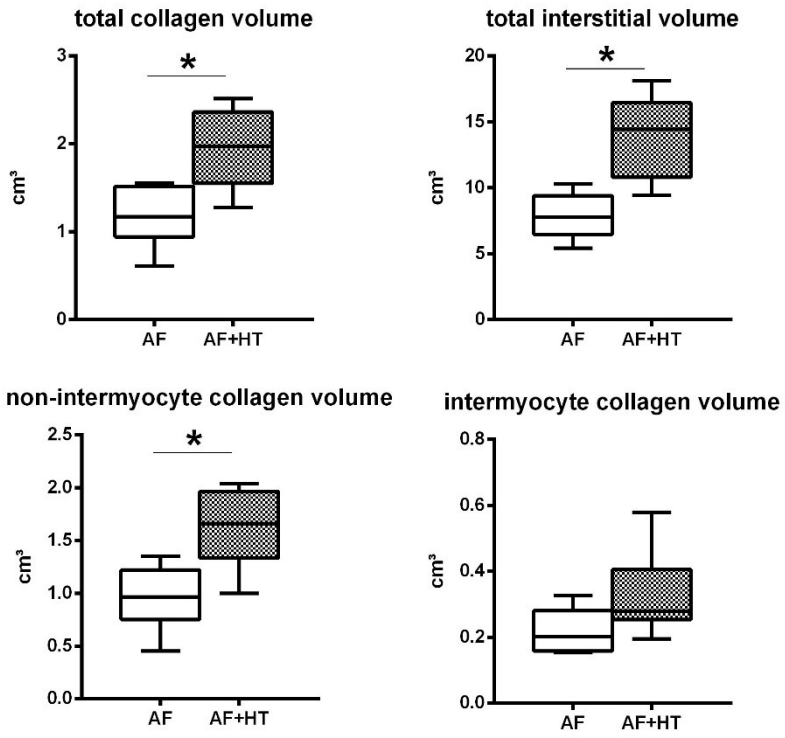

Figure 19. Structural changes in stereology. Intermyocyte collagen volume was comparable between both groups. Animals in AF+HT group had significantly higher total collagen, non-intermyocyte collagen volume and total interstitial volume

(p<0.05). This figure contains data from Manninger M et al., Heart Rhythm. 2018 Sep;15(9):1328-1336.(1)

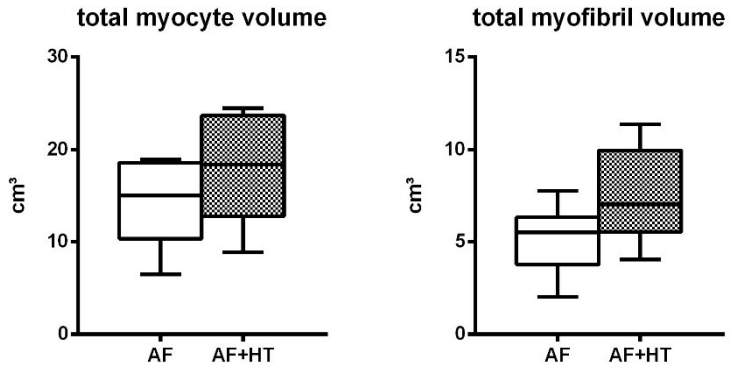

Figure 20. Cardiomyocyte remodelling in stereology. There was no significant difference in total myofibril or myocyte volumes between both groups (p=n.s.). This figure contains data from Manninger M et al., Heart Rhythm. 2018 Sep;15(9):1328-1336.(1)

In both LA and RA, distribution of connexin 43 was comparable between both groups (Figure 21). The ratio of signal intensity between lateral sides and z-discs was LA: 0.39±0.1 in the AF+HT group and 0.37±0.1 in the AF group in the LA (p=0.769) and 0.37±0.1 in the AF+HT group and 0.46±0.1 in the AF group in the RA (p=0.073).(1)

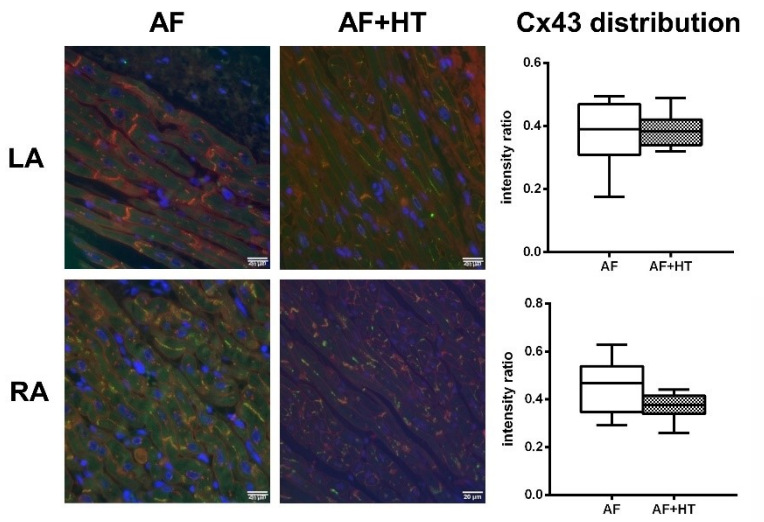

Figure 21. Connexin 43 distribution. Left panels, Representative images (immunofluorescence staining) of left (LA) and right (RA) atrial tissue of animals in the atrial fibrillation (AF) and AF + arterial hypertension (HT) group. Connexin 43 is stained green, cell membranes are stained red and nuclei are stained blue. Right panels, Signal intensity ratio between lateral sides and z-discs. There was no significant difference in distribution of connexin 43. This figure contains data from Manninger M et al., Heart Rhythm. 2018 Sep;15(9):1328-1336.(1)

3.2.4 Electrical remodelling

In closed-chest electrophysiological studies during the sacrifice experiment, AERP as well as APD90 in both left and right atria were comparable between both groups at every pacing cycle length from 400 to 200 ms (Figure 22).(1)

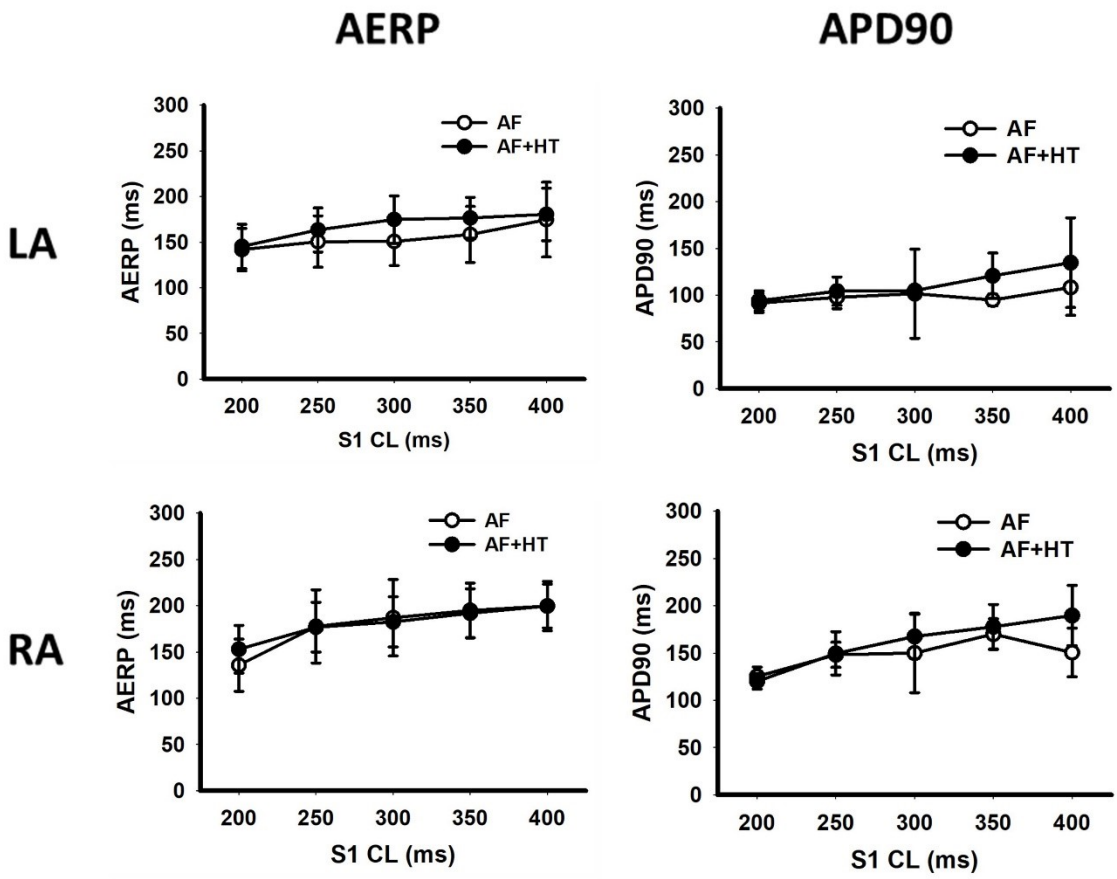

Figure 22. Electrical remodelling. There was no significant difference in refractory periods (left panels) or action potential durations (right panels) at S1 pacing cycle lengths from 400 to 200 ms between the atrial fibrillation (AF) group and AF + arterial hypertension (HT) group. This figure contains data from Manninger M et al., Heart Rhythm. 2018 Sep;15(9):1328-1336.(1)

Endocardial conduction velocities at a pacing cycle length of 600 ms were comparable between both groups in both left and right atria (Figure 23). Epicardial conduction velocities measured on the multielectrode array at pacing cycle lengths 250 to 500 ms were comparable between both groups in both left and right atria (Figure 24).(1)

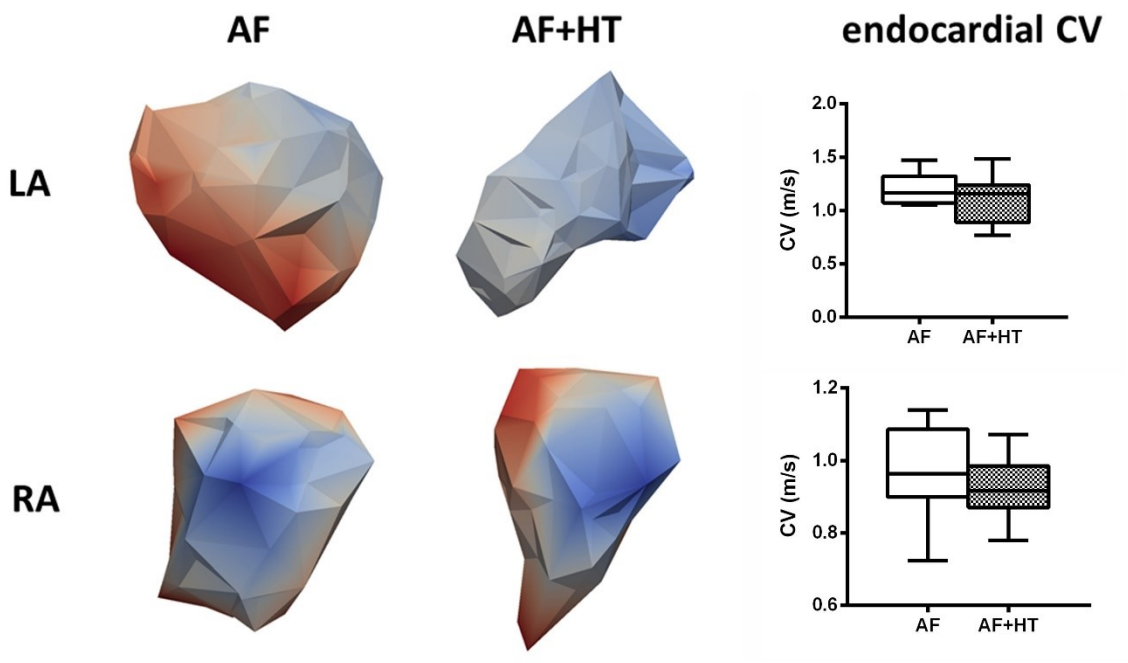

Figure 23. Endocardial conduction velocities (CV). Left panels, Representative propagation maps (S1 pacing cycle length = 600 ms) of the left (LA) and right (RA) atrium in animals in the atrial fibrillation (AF) group and AF + arterial hypertension (HT) group. Propagation maps are color coded from blue to red (earliest to latest activation). Right panels, Mean global CV showed no significant difference between both groups. This figure contains data from Manninger M et al., Heart Rhythm. 2018 Sep;15(9):1328-1336.(1)

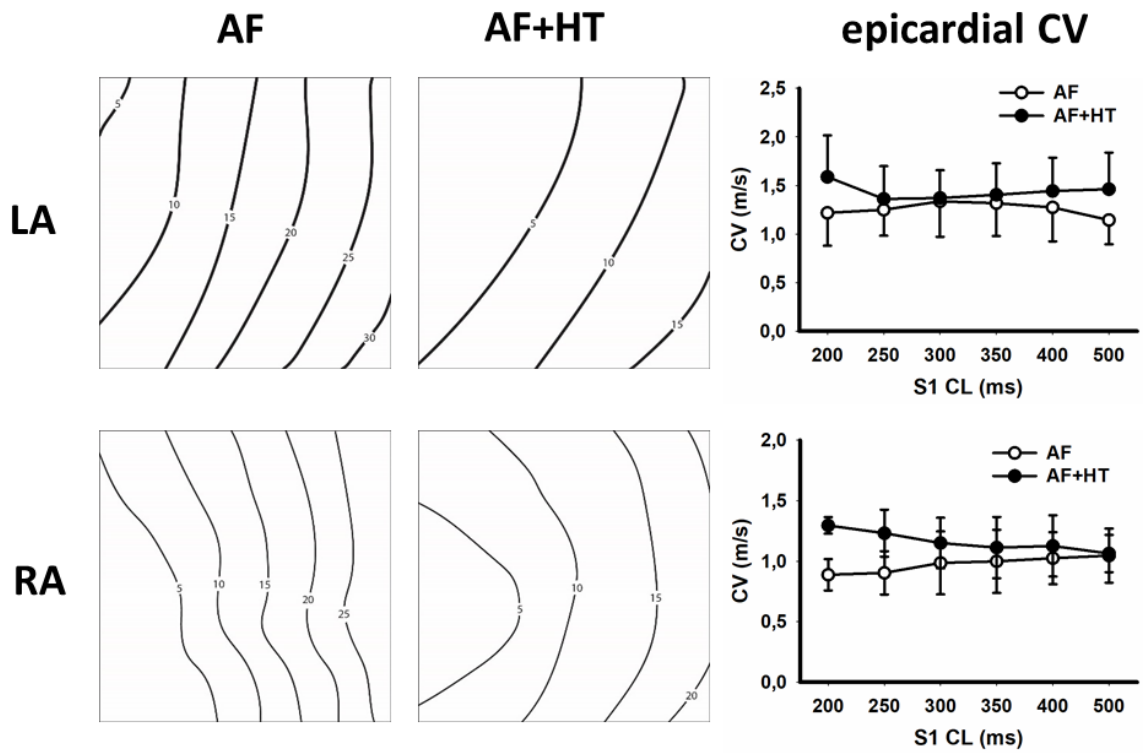

Figure 24. Epicardial conduction velocities (CV). Left panels, Representative propagation maps (S1 pacing cycle length = 400 ms, isochrones of 5 ms) of the left (LA) and right (RA) atrium in animals in the atrial fibrillation (AF) group and AF + arterial hypertension (HT) group. Right panels, Mean CV at S1 pacing cycle lengths between 500 and 200 ms showed no significant difference between both groups (p=n.s.). This figure contains data from Manninger M et al., Heart Rhythm. 2018 Sep;15(9):1328-1336.(1)

Mapping during AF in both atria showed no difference in complexity between both groups. Neither mean AF cycle length, nor waves per cycle length, endocardial breakthroughs per cycle length, mean conduction velocity during AF, maximum dissociation or fractionation were different between both groups (Figure 25, Figure 26, Table 2).(1)

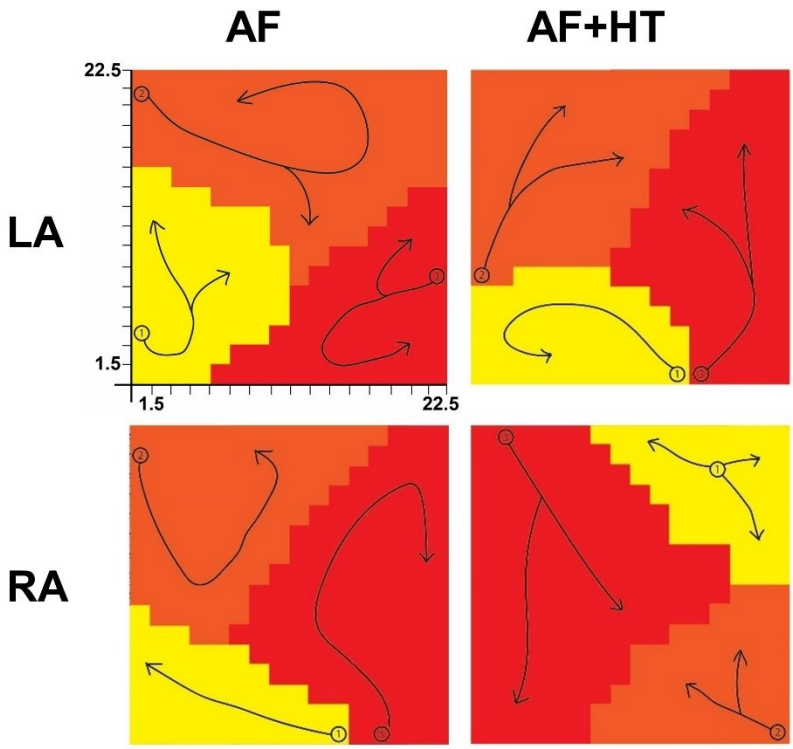

Figure 25. AF complexity mapping sample maps. Representative left (LA) and right (RA) atrial wave maps during AF in animals in the atrial fibrillation (AF) group and AF + arterial hypertension (HT) group. The scale indicates electrode distance in mm. This figure contains data from Manninger M et al., Heart Rhythm. 2018 Sep;15(9):1328-1336.(1)

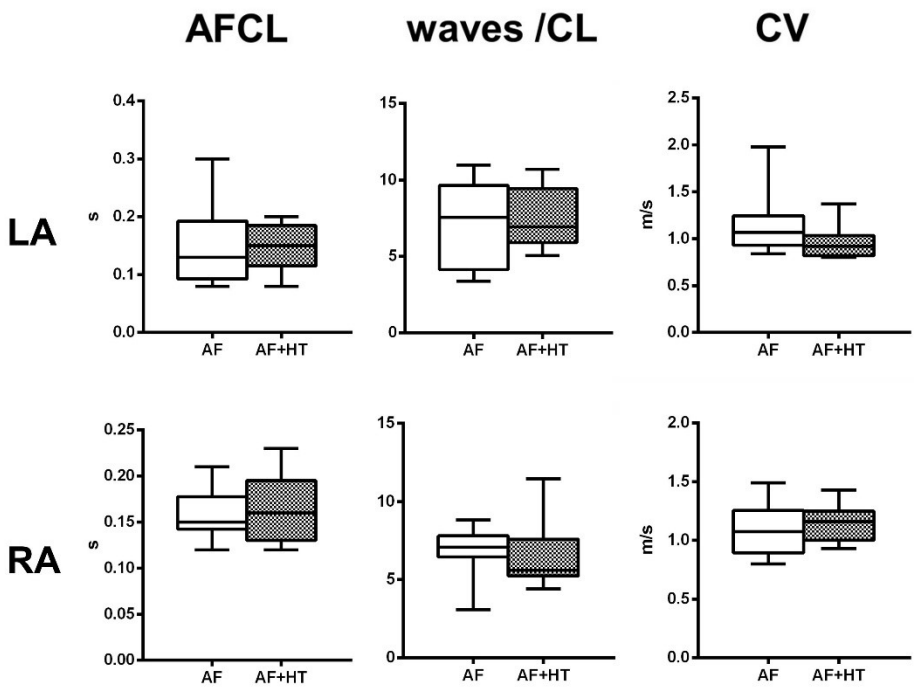

Figure 26. AF complexity mapping I. There were no differences in AF cycle length (AFCL), waves per cycle length and conduction velocity between both groups (p=n.s.). This figure contains data from Manninger M et al., Heart Rhythm. 2018 Sep;15(9):1328-1336.(1)

	AF+HT	AF	p
n	8	9	
LA: epicardial breakthroughs per cycle length	2.93±1.7	3.1±1.2	0.853
RA: epicardial breakthroughs per cycle length	2.46±1.3	2.71±1.0	0.668
LA: fractionation index	1.47±0.7	1.59±0.7	0.715
RA: fractionation index	1.13±0.7	0.98±0.3	0.564
LA: maximal dissociation (ms)	23.6±4.2	22.3±8.6	0.702
RA: maximal dissociation (ms)	17.5±6.6	19.6±5.3	0.490

Table 2. AF complexity mapping II. Epicardial left (LA) and right (RA) mapping during AF showed no difference in endocardial breakthroughs per cycle, fractionation or maximal dissociation between both groups. This table contains data from Manninger M et al., Heart Rhythm. 2018 Sep;15(9):1328-1336.(1)

3.2.5 Computer modelling

In a three-dimensional monolayer computational model using data from the electrophysiological studies as well as anatomical data from both groups, AF was induced by an S1-S2 protocol. AF duration was significantly longer in the AF+HT group than in the AF group (median AF duration: 610 (135-10000) ms in AF+HT vs. 216 (135-4925) ms in AF; p<0.0001; Figure 27).(1)

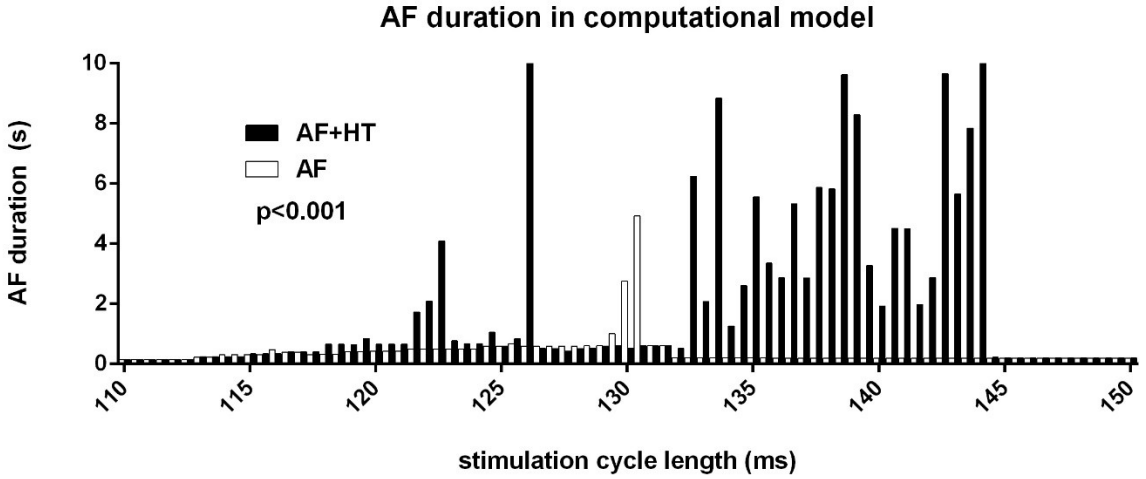

Figure 27. AF duration after induction in a three-dimensional computational model. In the AF+HT group (red), AF duration was significantly longer as compared to the AF group (blue, p<0.001). This figure contains data from Manninger M et al., Heart Rhythm. 2018 Sep;15(9):1328-1336.(1)

4 Discussion

4.1 Development of atrial fibrillation in the presence of arterial hypertension

We studied the impact of HT on the development of AF and could demonstrate, that DOCA-induced HT leads to concentric LV hypertrophy, atrial cardiomyocyte hypertrophy, impaired LA contractile function, each rendering the atria more susceptible to AF.

The DOCA model of hypertension is based on mineralocorticoid stimulation producing a sustained sodium- and volume-dependent elevation of arterial blood pressure.(237) As expected, after 12 weeks of DOCA treatment, pigs showed left ventricular remodelling (concentric hypertrophy), no clinical signs of heart failure, normal sinus rhythm and no spontaneous arrhythmias.

Among the different models of hypertensive heart disease, atrial enlargement is a common factor.(186, 198, 202, 203) It develops secondary to hypertension as an early event in the atrial remodelling process.(202, 203) Independent of other structural changes that may occur during hypertrophic remodelling, atrial substrate size per se is a contributing factor to AF stabilization.(125)

In other models, structural remodelling in hypertensive heart disease was characterized by atrial fibrosis and cardiomyocyte hypertrophy.(238-240) Cardiomyocyte hypertrophy was also present in our model after 12 weeks of DOCA treatment, but there were no signs for an increase in collagen content of the atria. This indicates that any arrhythmic potential in our model of hypertensive heart disease may most likely be located in the cardiomyocyte itself and fibrotic atrial remodelling is not necessary for increased AF vulnerability.(88) However, collagen content must not reflect myofibroblast activation. Since myofibroblasts may alter conduction, modify cardiomyocytes electrically and facilitate ectopic activity, there may be an early state of myofibroblast activation before fibrosis becomes apparent.(241)

In this study, we found that hypertensive remodelling lead to a reduced left atrial contractile function as suggested in past trials.(242) Results for right atrial function pointed towards the same direction, although, besides significant changes in right atrial end-diastolic volume, there was just a tendency of contractile dysfunction. This might be explained by the small number of animals in the group as well as by an analytical limitation, since borders between superior and inferior vena cava and right atrium cannot be drawn as easily in pigs as in humans due to the different anatomy of their insertion sites.

These findings could be confirmed in cellular measurements, where isolated atrial cardiomyocytes for pigs with hypertensive heart disease showed impaired contractility during field stimulation.(220) These findings suggest that arterial hypertension leads to reduced atrial contractility at the cellular level.

Experimental models of hypertension are not consistent in terms of electrical remodelling. Some studies report no change or shortening of the AERP, others an increased refractoriness. However, structural changes including cardiomyocyte hypertrophy and fibrosis are consistent in all reported studies.(186, 198, 202, 203)

Lau and colleagues characterized a sheep model of hypertension induced by the “one-kidney, one-clip” method (unilateral nephrectomy and clipping of the contralateral renal artery).(203) After a mean duration of 7 weeks, blood pressure almost doubled in the HT group (mean blood pressure: 176/119 vs. 95/62 mmHg). Hypertensive sheep had enlarged left atria, reduced left atrial function, higher AERP, slower conduction velocity, increased interstitial fibrosis and increased infiltration of inflammatory cells as compared to controls. In the same model, the group could also demonstrate electrostructural correlations between conduction abnormalities, AF inducibility and atrial inflammation and fibrosis.(202)

In another sheep model of arterial hypertension induced by prenatal corticosteroid exposure, the group of Kistler and colleagues showed that at the age of around 4.5 years, hypertensive sheep (mean blood pressure: 112/85 vs. 89/61 mmHg in controls) had unchanged AERP, but slower conduction velocities, increased AF inducibility, increased atrial collagen content, increased apoptosis and cardiomyocyte hypertrophy as compared to healthy controls.(186)

In spontaneously hypertensive rats at the age of 12 months, higher blood pressure (mean systolic blood pressure: 191±32 vs. 128±16 mmHg in controls) was associated with shortened AERP, increased conduction heterogeneity, increased AF inducibility and increased fibrosis.(198)

In our model, we did not observe changes in atrial refractory period in hypertensive heart disease. In animal models, where AERP remained unchanged, such as in sheep with HT induced by prenatal corticosteroid exposure or dogs with tachypacing-induced chronic heart failure, higher AF stability was associated with conduction abnormalities, most likely caused by structural remodelling.(85, 117, 186) Characteristics of structural and electrical remodelling differ between species and models, pointing out that there are various forms or remodelling and AERP is only one of the contributing factors. In our model, AF was more likely to be induced in animals with hypertensive heart disease which indicates that hypertensive remodelling represents an arrhythmic substrate.

In contrast to other animal models of hypertensive heart disease, there was no increase in atrial fibrosis in our model. This might be due to the different aetiologies, duration and severity of hypertension as well as the different species used.(186, 198, 202, 203) In a very similar porcine model of 12 and 18 weeks of DOCA exposure combined with angiotensin II treatment, Sun et al. found an increase in left atrial fibrosis.(243) The method of quantification of fibrosis is not consistent throughout the different studies, thus we chose to perform stereological analyses for the second series focusing on the role of HT in the presence of AF.(228)

Since the underlying mechanism for this arrhythmogenicity is most likely located within the cardiomyocyte, changes may be reversible and serve as promising therapeutic targets to prevent the development and progression of AF.

Possible triggers for these functional changes may be increased atrial filling pressures and volume overload as suggested by the increased atrial size.

4.2 Progression of atrial fibrillation in the presence of arterial hypertension

We studied the impact of arterial hypertension on early arrhythmia progression in a porcine model with RAP-induced AF. In prior studies in porcine model of DOCA-induced HT, we could show that the presence of HT increases AF stability.(218) Here, we could show, that this increased stability is not supported by electrophysiological changes and is likely not due to the observed increase in fibrosis, since conduction velocities and AF complexity did not differ between both groups. The main structural change caused by HT was atrial dilatation, which seems to be sufficient to increase AF stability. In this early phase of AF stabilisation, HT facilitates AF by atrial dilatation.

Prior animal studies have shown that remodelling during the development and progression of AF consists of the early electrical remodelling, which is characterized by shortening of the APD, shortening of the AERP and loss of rate adaption of the AERP as well as a "second factor" that is most likely characterized by more gradual structural remodelling.(85, 86) Atrial fibrosis, cardiomyocyte hypertrophy, and rearrangement of connexins and changes in atrial architecture (dilation, altered composition of the extracellular matrix, endo-epicardial dissociation) are some of the described structural changes that contribute to the development and progression of AF.(17, 87)

4.2.1 Atrial fibrosis

Risk factors such as HT favour transition from paroxysmal to persistent AF by accelerating structural remodelling and/or increasing complexity of the substrate.(17) There are strong indications from animal studies that fibrosis can promote arrhythmias, but in human studies, the association between AF and fibrosis is nonlinear and complex.(244, 245) Atrial biopsies of patients with AF as well as risk factors for AF such as valvular heart disease, hypertrophic cardiomyopathy, dilated cardiomyopathy and advanced age showed increased atrial fibrosis.(246-

248) Fibrosis is thought to cause endo-epicardial dissociation as well as slow and discontinuous conduction.(249, 250) In a goat model of AF, inter-myocyte fibrosis developed over months without changing non-intermyocyte collagen content.(88) When exposing AF animals to HT, we observed early changes in collagen distribution and collagen content. The extent of fibrosis observed in our model is comparable to the model of dogs with heart failure, although the quality of fibrosis differs. In the dog model, the pattern and pathogenesis are more consistent with replacement fibrosis secondary to myocyte death (increased myocyte apoptosis and necrosis in the hours-days immediately after the start of ventricular pacing).(117)

Epicardial multielectrode array mapping in goats with short vs. long term (3 weeks vs. 6 months) AF induced by RAP showed that increased AF stability during the progression of AF (as measured by AAD refractoriness) was associated with an increased AF complexity as measured by AF cycle length, number of simultaneous waves and incidence of conduction block.(88) In many animal models, increased AF stability was associated with a reduction in conduction velocity.(88, 186, 202, 203) In our model, adding HT did not lead to a further increase in AF complexity or further conduction velocity reduction. We speculate that this is due to the short duration of RAP (two weeks) with relatively short episodes of sustained AF after pausing RAP. In this early stage, alterations in atrial architecture might be sufficient to maintain the arrhythmia. Also, increased atrial collagen content need not necessarily be associated with an increase in AF complexity.(251) While prior studies showed that AF complexity is a marker of AF progression and is associated with intermyocyte fibrosis, the exact association between AF complexity and non-intermyocyte fibrosis (as measured in our study) remains unclear.(88, 113) We speculate that not quantity of fibrosis, but rather quality and distribution have the greatest impact in arrhythmogenic altering of conduction. Fibrosis seems not to have a strong impact on AF stability in this model, since AF complexity in multielectrode array mapping as well as distribution of connexin 43 were unaltered.

4.2.2 Atrial cardiomyocyte hypertrophy

Experimental studies in rats with secondary hyperaldosteronism as well as animal models of atrial dilatation, chronic heart failure and RAP have suggested cardiomyocyte hypertrophy as a favouring factor in development and progression of AF.(117, 125, 238, 252, 253) Using stereology, the gold standard for quantitative histological assessment, we could show that total atrial cardiomyocyte volume was not different between AF animals with and without HT. The fact that echocardiography revealed significant left ventricular hypertrophy in the AF+HT model indicates that atrial cardiomyocyte hypertrophy might develop secondarily to atrial fibrosis and dilatation. Therefore, in this early phase of HT, atrial hypertrophy might not play an important role in attenuating AF.

4.2.3 Atrial dilatation

In this model, increased intraventricular pressures lead to atrial dilatation. In prior studies in animals subjected to DOCA, we could demonstrate a leftward shift of the end diastolic pressure volume relationship.(219) The fact that neither LA pressures, nor LV end diastolic pressures were different between both groups can be explained by the fact that animals were kept in deep anaesthesia throughout the sacrifice experiment.

The role of acute and chronic atrial dilatation on the development and perpetuation of AF has been extensively studied in various animal models. The factors contributing to the AF substrate differed between the models and included increase in fibrosis, cardiomyocyte hypertrophy, connexin redistribution as well as atrial size per se (atrial geometry), while the coherent finding was that atrial dilatation causes increased AF stability. In a dog model of mitral regurgitation, increased vulnerability to AF was caused by structural changes including fibrosis leading to increased heterogeneity of conduction revealed by optical mapping.(121, 123) In a goat model of complete AV block, increased AF stability and atrial dilatation led to atrial cardiomyocyte hypertrophy without fibrosis increase and did not affect AERP or

dispersion of AERP.(125) In contrast to the histological substrate in the AV-block goats, HT resulted in non-intermyocyte fibrosis without atrial cardiomyocyte hypertrophy in our model. The fact that atrial size alone may facilitate AF perpetuation was supported by simulations in a two-dimensional computational model of a canine atrium.(254) This could be verified in our mathematical model incorporating electrophysiological data as well as anatomical data from the in vivo model.

4.2.4 Clinical implication

It has been suggested by observational studies in humans that aldosterone plays a key role in atrial remodelling in patients with arterial hypertension.(255, 256) However, patients included in these studies suffer from multiple comorbidities, which makes it difficult to determine, whether the effects of aldosterone per se triggers AF or only in presence of structural heart disease. Mineralocorticoid receptor (MR) agonists have been more effective in preventing AF than placebo in a post-hoc analysis of the multicentre EMPHASIS-HF study (Eplerenone in Mild Patients Hospitalization and Survival Study in Heart Failure).(257) Further clinical studies need to be conducted to answer the question, whether MRs might also play a role in preventing the development and progression of AF.

The fact that HT is a trigger and promotor of AF underlines the importance of strict blood pressure control in AF patients. We believe that the extent of pre-existing structural remodelling is an important determinant for the effect of upstream therapy.

4.3 Summary

In our study, HT was associated with concentric left ventricular hypertrophy, increased myocardial mass, atrial cardiomyocyte hypertrophy, increased left atrial volumes, decreased total and active left atrial ejection fraction and increased AF inducibility, while AERP and atrial fibrosis were unchanged.

In the presence of AF, HT was associated with atrial dilatation, an increase in left atrial non-intermyocyte fibrosis, increased left and right atrial weights and increased AF stability, while AERP, ADP90, conduction velocities and AF complexity were unchanged.

Increased atrial fibrosis was absent after twelve weeks in our porcine model of DOCA-induced HT without RAP.(219) The fact that the combination of AF+HT leads to this accumulation of collagen indicates that HT triggers profibrotic pathways in the presence of AF. However, at this early state, fibrosis seems not to be the key component increasing AF stability, since neither conduction velocities, nor AF complexity were different between both groups in this study. In the computational model, we could show that increased AF stability in this model can be explained solely by atrial dilatation.

5 Conclusion

DOCA-induced HT increases atrial susceptibility towards fibrillation at a state of impaired left atrial contractile function in the absence of increased fibrosis, suggesting functional alteration at the cellular level. The underlying mechanisms in this model may therefore be reversible and serve as therapeutic targets to prevent the development and progression of AF.

DOCA-induced HT favours AF progression by increasing AF stability by early structural remodelling including atrial dilatation and fibrosis, but not by atrial cardiomyocyte hypertrophy, AF complexity, changes in refractory periods or action potential durations. These structural changes are sufficient to increase AF stability, emphasizing the importance of strict blood pressure control in AF patients.

6 Bibliography

1. Manninger M, Zweiker D, van Hunnik A, Alogna A, Prassl AJ, Schipke J, et al. Arterial hypertension drives arrhythmia progression via specific structural remodeling in a porcine model of atrial fibrillation. Heart Rhythm. 2018;15(9):1328-36.
2. Kirchhof P, Benussi S, Kotecha D, Ahlsson A, Atar D, Casadei B, et al. 2016 ESC Guidelines for the management of atrial fibrillation developed in collaboration with EACTS. Eur Heart J. 2016;37(38):2893-962.
3. Go AS, Hylek EM, Phillips KA, Chang Y, Henault LE, Selby JV, et al. Prevalence of diagnosed atrial fibrillation in adults: national implications for rhythm management and stroke prevention: the AnTicoagulation and Risk Factors in Atrial Fibrillation (ATRIA) Study. JAMA. 2001;285(18):2370-5.
4. Lloyd-Jones DM, Wang TJ, Leip EP, Larson MG, Levy D, Vasan RS, et al. Lifetime risk for development of atrial fibrillation: the Framingham Heart Study. Circulation. 2004;110(9):1042-6.
5. Heeringa J, van der Kuip DA, Hofman A, Kors JA, van Herpen G, Stricker BH, et al. Prevalence, incidence and lifetime risk of atrial fibrillation: the Rotterdam study. Eur Heart J. 2006;27(8):949-53.
6. Kannel WB, Wolf PA, Benjamin EJ, Levy D. Prevalence, incidence, prognosis, and predisposing conditions for atrial fibrillation: population-based estimates. Am J Cardiol. 1998;82(8A):2N-9N.
7. Wolf PA, Abbott RD, Kannel WB. Atrial fibrillation as an independent risk factor for stroke: the Framingham Study. Stroke. 1991;22(8):983-8.
8. Lin HJ, Wolf PA, Kelly-Hayes M, Beiser AS, Kase CS, Benjamin EJ, et al. Stroke severity in atrial fibrillation. The Framingham Study. Stroke. 1996;27(10):1760-4.
9. Gottdiener JS, Arnold AM, Aurigemma GP, Polak JF, Tracy RP, Kitzman DW, et al. Predictors of congestive heart failure in the elderly: the Cardiovascular Health Study. J Am Coll Cardiol. 2000;35(6):1628-37.
10. Wattigney WA, Mensah GA, Croft JB. Increasing trends in hospitalization for atrial fibrillation in the United States, 1985 through 1999: implications for primary prevention. Circulation. 2003;108(6):711-6.

11. Benjamin EJ, Wolf PA, D'Agostino RB, Silbershatz H, Kannel WB, Levy D. Impact of atrial fibrillation on the risk of death: the Framingham Heart Study. Circulation. 1998;98(10):946-52.
12. Nieuwlaat R, Capucci A, Camm AJ, Olsson SB, Andresen D, Davies DW, et al. Atrial fibrillation management: a prospective survey in ESC member countries: the Euro Heart Survey on Atrial Fibrillation. Eur Heart J. 2005;26(22):2422-34.
13. Corley SD, Epstein AE, DiMarco JP, Domanski MJ, Geller N, Greene HL, et al. Relationships between sinus rhythm, treatment, and survival in the Atrial Fibrillation Follow-Up Investigation of Rhythm Management (AFFIRM) Study. Circulation. 2004;109(12):1509-13.
14. Roy D, Talajic M, Nattel S, Wyse DG, Dorian P, Lee KL, et al. Rhythm control versus rate control for atrial fibrillation and heart failure. N Engl J Med. 2008;358(25):2667-77.
15. Van Gelder IC, Hagens VE, Bosker HA, Kingma JH, Kamp O, Kingma T, et al. A comparison of rate control and rhythm control in patients with recurrent persistent atrial fibrillation. N Engl J Med. 2002;347(23):1834-40.
16. Stewart S, Murphy NF, Walker A, McGuire A, McMurray JJ. Cost of an emerging epidemic: an economic analysis of atrial fibrillation in the UK. Heart. 2004;90(3):286-92.
17. Schotten U, Verheule S, Kirchhof P, Goette A. Pathophysiological mechanisms of atrial fibrillation: a translational appraisal. Physiol Rev. 2011;91(1):265-325.
18. Manolis AJ, Hamodraka ES, Poulimenos LE. Electrocardiography for the diagnosis of left ventricular hypertrophy: revisiting an old friend in times of austerity. J Hypertens. 2012;30(7):1325-7.
19. Schneider MP, Hua TA, Bohm M, Wachtell K, Kjeldsen SE, Schmieder RE. Prevention of atrial fibrillation by Renin-Angiotensin system inhibition a meta-analysis. J Am Coll Cardiol. 2010;55(21):2299-307.
20. Goette A, Staack T, Rocken C, Arndt M, Geller JC, Huth C, et al. Increased expression of extracellular signal-regulated kinase and angiotensin-converting enzyme in human atria during atrial fibrillation. J Am Coll Cardiol. 2000;35(6):1669-77.

21. Jibrini MB, Molnar J, Arora RR. Prevention of atrial fibrillation by way of abrogation of the renin-angiotensin system: a systematic review and meta-analysis. Am J Ther. 2008;15(1):36-43.
22. Wachtell K, Lehto M, Gerdts E, Olsen MH, Hornestam B, Dahlof B, et al. Angiotensin II receptor blockade reduces new-onset atrial fibrillation and subsequent stroke compared to atenolol: the Losartan Intervention For End Point Reduction in Hypertension (LIFE) study. J Am Coll Cardiol. 2005;45(5):712-9.
23. Schoen T, Pradhan AD, Albert CM, Conen D. Type 2 diabetes mellitus and risk of incident atrial fibrillation in women. J Am Coll Cardiol. 2012;60(15):1421-8.
24. Du X, Ninomiya T, de Galan B, Abadir E, Chalmers J, Pillai A, et al. Risks of cardiovascular events and effects of routine blood pressure lowering among patients with type 2 diabetes and atrial fibrillation: results of the ADVANCE study. Eur Heart J. 2009;30(9):1128-35.
25. Rizzo MR, Sasso FC, Marfella R, Siniscalchi M, Paolisso P, Carbonara O, et al. Autonomic dysfunction is associated with brief episodes of atrial fibrillation in type 2 diabetes. J Diabetes Complications. 2015;29(1):88-92.
26. Chung MK, Martin DO, Sprecher D, Wazni O, Kanderian A, Carnes CA, et al. C-reactive protein elevation in patients with atrial arrhythmias: inflammatory mechanisms and persistence of atrial fibrillation. Circulation. 2001;104(24):2886-91.
27. Donath MY, Shoelson SE. Type 2 diabetes as an inflammatory disease. Nat Rev Immunol. 2011;11(2):98-107.
28. Ziolo MT, Mohler PJ. Defining the role of oxidative stress in atrial fibrillation and diabetes. J Cardiovasc Electrophysiol. 2015;26(2):223-5.
29. Fatemi O, Yuriditsky E, Tsioufis C, Tsachris D, Morgan T, Basile J, et al. Impact of intensive glycemic control on the incidence of atrial fibrillation and associated cardiovascular outcomes in patients with type 2 diabetes mellitus (from the Action to Control Cardiovascular Risk in Diabetes Study). Am J Cardiol. 2014;114(8):1217-22.
30. Chang CH, Chang YC, Wu LC, Lin JW, Chuang LM, Lai MS. Different angiotensin receptor blockers and incidence of diabetes: a nationwide population-based cohort study. Cardiovasc Diabetol. 2014;13:91.
31. Nguyen TD, Shingu Y, Amorim PA, Schwarzer M, Doenst T. Glucagon-like peptide-1 reduces contractile function and fails to boost glucose utilization in normal hearts in the presence of fatty acids. Int J Cardiol. 2013;168(4):4085-92.

32. Huxley RR, Misialek JR, Agarwal SK, Loehr LR, Soliman EZ, Chen LY, et al. Physical activity, obesity, weight change, and risk of atrial fibrillation: the Atherosclerosis Risk in Communities study. Circ Arrhythm Electrophysiol. 2014;7(4):620-5.

33. Murphy NF, MacIntyre K, Stewart S, Hart CL, Hole D, McMurray JJ. Long-term cardiovascular consequences of obesity: 20-year follow-up of more than 15 000 middle-aged men and women (the Renfrew-Paisley study). Eur Heart J. 2006;27(1):96-106.

34. Wanahita N, Messerli FH, Bangalore S, Gami AS, Somers VK, Steinberg JS. Atrial fibrillation and obesity--results of a meta-analysis. Am Heart J. 2008;155(2):310-5.

35. Wang TJ, Parise H, Levy D, D'Agostino RB, Sr., Wolf PA, Vasan RS, et al. Obesity and the risk of new-onset atrial fibrillation. JAMA. 2004;292(20):2471-7.

36. Overvad TF, Rasmussen LH, Skjoth F, Overvad K, Lip GY, Larsen TB. Body mass index and adverse events in patients with incident atrial fibrillation. Am J Med. 2013;126(7):640 e9-17.

37. Karason K, Molgaard H, Wikstrand J, Sjostrom L. Heart rate variability in obesity and the effect of weight loss. Am J Cardiol. 1999;83(8):1242-7.

38. Visser M, Bouter LM, McQuillan GM, Wener MH, Harris TB. Elevated C-reactive protein levels in overweight and obese adults. JAMA. 1999;282(22):2131-5.

39. Russo C, Jin Z, Homma S, Rundek T, Elkind MS, Sacco RL, et al. Effect of obesity and overweight on left ventricular diastolic function: a community-based study in an elderly cohort. J Am Coll Cardiol. 2011;57(12):1368-74.

40. Abed HS, Wittert GA, Leong DP, Shirazi MG, Bahrami B, Middeldorp ME, et al. Effect of weight reduction and cardiometabolic risk factor management on symptom burden and severity in patients with atrial fibrillation: a randomized clinical trial. JAMA. 2013;310(19):2050-60.

41. Pathak RK, Elliott A, Middeldorp ME, Meredith M, Mehta AB, Mahajan R, et al. Impact of CARDIOrespiratory FITness on Arrhythmia Recurrence in Obese Individuals With Atrial Fibrillation: The CARDIO-FIT Study. J Am Coll Cardiol. 2015;66(9):985-96.

42. Pathak RK, Middeldorp ME, Lau DH, Mehta AB, Mahajan R, Twomey D, et al. Aggressive risk factor reduction study for atrial fibrillation and implications for the

outcome of ablation: the ARREST-AF cohort study. J Am Coll Cardiol. 2014;64(21):2222-31.

43. Pathak RK, Middeldorp ME, Meredith M, Mehta AB, Mahajan R, Wong CX, et al. Long-Term Effect of Goal-Directed Weight Management in an Atrial Fibrillation Cohort: A Long-Term Follow-Up Study (LEGACY). J Am Coll Cardiol. 2015;65(20):2159-69.

44. Benjamin EJ, Levy D, Vaziri SM, D'Agostino RB, Belanger AJ, Wolf PA. Independent risk factors for atrial fibrillation in a population-based cohort. The Framingham Heart Study. JAMA. 1994;271(11):840-4.

45. Spach MS, Miller WT, 3rd, Dolber PC, Kootsey JM, Sommer JR, Mosher CE, Jr. The functional role of structural complexities in the propagation of depolarization in the atrium of the dog. Cardiac conduction disturbances due to discontinuities of effective axial resistivity. Circ Res. 1982;50(2):175-91.

46. Hayashi H, Wang C, Miyauchi Y, Omichi C, Pak HN, Zhou S, et al. Aging-related increase to inducible atrial fibrillation in the rat model. J Cardiovasc Electrophysiol. 2002;13(8):801-8.

47. Koura T, Hara M, Takeuchi S, Ota K, Okada Y, Miyoshi S, et al. Anisotropic conduction properties in canine atria analyzed by high-resolution optical mapping: preferential direction of conduction block changes from longitudinal to transverse with increasing age. Circulation. 2002;105(17):2092-8.

48. Anyukhovsky EP, Sosunov EA, Chandra P, Rosen TS, Boyden PA, Danilo P, Jr., et al. Age-associated changes in electrophysiologic remodeling: a potential contributor to initiation of atrial fibrillation. Cardiovasc Res. 2005;66(2):353-63.

49. Anyukhovsky EP, Sosunov EA, Plotnikov A, Gainullin RZ, Jhang JS, Marboe CC, et al. Cellular electrophysiologic properties of old canine atria provide a substrate for arrhythmogenesis. Cardiovasc Res. 2002;54(2):462-9.

50. Guha K, McDonagh T. Heart failure epidemiology: European perspective. Curr Cardiol Rev. 2013;9(2):123-7.

51. Braunschweig F, Cowie MR, Auricchio A. What are the costs of heart failure? Europace. 2011;13 Suppl 2:ii13-7.

52. Wodchis WP, Bhatia RS, Leblanc K, Meshkat N, Morra D. A review of the cost of atrial fibrillation. Value Health. 2012;15(2):240-8.

53. Kotecha D, Piccini JP. Atrial fibrillation in heart failure: what should we do? Eur Heart J. 2015;36(46):3250-7.

54. Wang TJ, Larson MG, Levy D, Vasan RS, Leip EP, Wolf PA, et al. Temporal relations of atrial fibrillation and congestive heart failure and their joint influence on mortality: the Framingham Heart Study. Circulation. 2003;107(23):2920-5.
55. Olsson LG, Swedberg K, Ducharme A, Granger CB, Michelson EL, McMurray JJ, et al. Atrial fibrillation and risk of clinical events in chronic heart failure with and without left ventricular systolic dysfunction: results from the Candesartan in Heart failure-Assessment of Reduction in Mortality and morbidity (CHARM) program. J Am Coll Cardiol. 2006;47(10):1997-2004.
56. Kotecha D, Chudasama R, Lane DA, Kirchhof P, Lip GY. Atrial fibrillation and heart failure due to reduced versus preserved ejection fraction: A systematic review and meta-analysis of death and adverse outcomes. Int J Cardiol. 2016;203:660-6.
57. Mamas MA, Caldwell JC, Chacko S, Garratt CJ, Fath-Ordoubadi F, Neyses L. A meta-analysis of the prognostic significance of atrial fibrillation in chronic heart failure. Eur J Heart Fail. 2009;11(7):676-83.
58. Kirchhof P, Benussi S, Kotecha D, Ahlsson A, Atar D, Casadei B, et al. 2016 ESC Guidelines for the management of atrial fibrillation developed in collaboration with EACTS: The Task Force for the management of atrial fibrillation of the European Society of Cardiology (ESC)Developed with the special contribution of the European Heart Rhythm Association (EHRA) of the ESCEndorsed by the European Stroke Organisation (ESO). Eur Heart J. 2016.
59. Marrouche NF, Brachmann J, Andresen D, Siebels J, Boersma L, Jordaens L, et al. Catheter Ablation for Atrial Fibrillation with Heart Failure. N Engl J Med. 2018;378(5):417-27.
60. Nabauer M, Gerth A, Limbourg T, Schneider S, Oeff M, Kirchhof P, et al. The Registry of the German Competence NETwork on Atrial Fibrillation: patient characteristics and initial management. Europace. 2009;11(4):423-34.
61. Vahanian A, Otto CM. Risk stratification of patients with aortic stenosis. Eur Heart J. 2010;31(4):416-23.
62. Furberg CD, Psaty BM, Manolio TA, Gardin JM, Smith VE, Rautaharju PM. Prevalence of atrial fibrillation in elderly subjects (the Cardiovascular Health Study). Am J Cardiol. 1994;74(3):236-41.
63. Moretti M, Fabris E, Morosin M, Merlo M, Barbati G, Pinamonti B, et al. Prognostic significance of atrial fibrillation and severity of symptoms of heart failure

in patients with low gradient aortic stenosis and preserved left ventricular ejection fraction. Am J Cardiol. 2014;114(11):1722-8.

64. Messika-Zeitoun D, Bellamy M, Avierinos JF, Breen J, Eusemann C, Rossi A, et al. Left atrial remodelling in mitral regurgitation--methodologic approach, physiological determinants, and outcome implications: a prospective quantitative Doppler-echocardiographic and electron beam-computed tomographic study. Eur Heart J. 2007;28(14):1773-81.

65. Calvo N, Bisbal F, Guiu E, Ramos P, Nadal M, Tolosana JM, et al. Impact of atrial fibrillation-induced tachycardiomyopathy in patients undergoing pulmonary vein isolation. Int J Cardiol. 2013;168(4):4093-7.

66. Edner M, Caidahl K, Bergfeldt L, Darpo B, Edvardsson N, Rosenqvist M. Prospective study of left ventricular function after radiofrequency ablation of atrioventricular junction in patients with atrial fibrillation. Br Heart J. 1995;74(3):261-7.

67. Gertz ZM, Raina A, Saghy L, Zado ES, Callans DJ, Marchlinski FE, et al. Evidence of atrial functional mitral regurgitation due to atrial fibrillation: reversal with arrhythmia control. J Am Coll Cardiol. 2011;58(14):1474-81.

68. Zhou X, Otsuji Y, Yoshifuku S, Yuasa T, Zhang H, Takasaki K, et al. Impact of atrial fibrillation on tricuspid and mitral annular dilatation and valvular regurgitation. Circ J. 2002;66(10):913-6.

69. Ring L, Dutka DP, Wells FC, Fynn SP, Shapiro LM, Rana BS. Mechanisms of atrial mitral regurgitation: insights using 3D transoesophageal echo. Eur Heart J Cardiovasc Imaging. 2014;15(5):500-8.

70. Vizzardi E, Curnis A, Latini MG, Salghetti F, Rocco E, Lupi L, et al. Risk factors for atrial fibrillation recurrence: a literature review. J Cardiovasc Med (Hagerstown). 2014;15(3):235-53.

71. Digby GC, Baranchuk A. Sleep apnea and atrial fibrillation; 2012 update. Curr Cardiol Rev. 2012;8(4):265-72.

72. Lin YK, Lai MS, Chen YC, Cheng CC, Huang JH, Chen SA, et al. Hypoxia and reoxygenation modulate the arrhythmogenic activity of the pulmonary vein and atrium. Clin Sci (Lond). 2012;122(3):121-32.

73. Linz D. Atrial fibrillation in obstructive sleep apnea: atrial arrhythmogenic substrate of a different sort. Am J Cardiol. 2012;110(7):1071.

74. Patel D, Mohanty P, Di Biase L, Shaheen M, Lewis WR, Quan K, et al. Safety and efficacy of pulmonary vein antral isolation in patients with obstructive sleep apnea: the impact of continuous positive airway pressure. Circ Arrhythm Electrophysiol. 2010;3(5):445-51.
75. Naruse Y, Tada H, Satoh M, Yanagihara M, Tsuneoka H, Hirata Y, et al. Concomitant obstructive sleep apnea increases the recurrence of atrial fibrillation following radiofrequency catheter ablation of atrial fibrillation: clinical impact of continuous positive airway pressure therapy. Heart Rhythm. 2013;10(3):331-7.
76. Li L, Wang ZW, Li J, Ge X, Guo LZ, Wang Y, et al. Efficacy of catheter ablation of atrial fibrillation in patients with obstructive sleep apnoea with and without continuous positive airway pressure treatment: a meta-analysis of observational studies. Europace. 2014;16(9):1309-14.
77. Fein AS, Shvilkin A, Shah D, Haffajee CI, Das S, Kumar K, et al. Treatment of obstructive sleep apnea reduces the risk of atrial fibrillation recurrence after catheter ablation. J Am Coll Cardiol. 2013;62(4):300-5.
78. Hart RG, Eikelboom JW, Brimble KS, McMurtry MS, Ingram AJ. Stroke prevention in atrial fibrillation patients with chronic kidney disease. Can J Cardiol. 2013;29(7 Suppl):S71-8.
79. Roldan V, Marin F, Fernandez H, Manzano-Fernandez S, Gallego P, Valdes M, et al. Renal impairment in a "real-life" cohort of anticoagulated patients with atrial fibrillation (implications for thromboembolism and bleeding). Am J Cardiol. 2013;111(8):1159-64.
80. Gage BF, Waterman AD, Shannon W, Boechler M, Rich MW, Radford MJ. Validation of clinical classification schemes for predicting stroke: results from the National Registry of Atrial Fibrillation. JAMA. 2001;285(22):2864-70.
81. Kerr CR, Humphries KH, Talajic M, Klein GJ, Connolly SJ, Green M, et al. Progression to chronic atrial fibrillation after the initial diagnosis of paroxysmal atrial fibrillation: results from the Canadian Registry of Atrial Fibrillation. Am Heart J. 2005;149(3):489-96.
82. Jahangir A, Lee V, Friedman PA, Trusty JM, Hodge DO, Kopecky SL, et al. Long-term progression and outcomes with aging in patients with lone atrial fibrillation: a 30-year follow-up study. Circulation. 2007;115(24):3050-6.
83. European Heart Rhythm A, European Association for Cardio-Thoracic S, Camm AJ, Kirchhof P, Lip GY, Schotten U, et al. Guidelines for the management of

atrial fibrillation: the Task Force for the Management of Atrial Fibrillation of the European Society of Cardiology (ESC). Eur Heart J. 2010;31(19):2369-429.

84. Wyse DG, Gersh BJ. Atrial fibrillation: a perspective: thinking inside and outside the box. Circulation. 2004;109(25):3089-95.

85. Wijffels MC, Kirchhof CJ, Dorland R, Allessie MA. Atrial fibrillation begets atrial fibrillation. A study in awake chronically instrumented goats. Circulation. 1995;92(7):1954-68.

86. Stiles MK, John B, Wong CX, Kuklik P, Brooks AG, Lau DH, et al. Paroxysmal lone atrial fibrillation is associated with an abnormal atrial substrate: characterizing the "second factor". J Am Coll Cardiol. 2009;53(14):1182-91.

87. Nattel S. New ideas about atrial fibrillation 50 years on. Nature. 2002;415(6868):219-26.

88. Verheule S, Tuyls E, van Hunnik A, Kuiper M, Schotten U, Allessie M. Fibrillatory conduction in the atrial free walls of goats in persistent and permanent atrial fibrillation. Circ Arrhythm Electrophysiol. 2010;3(6):590-9.

89. Maesen B, Zeemering S, Afonso C, Eckstein J, Burton RA, van Hunnik A, et al. Rearrangement of atrial bundle architecture and consequent changes in anisotropy of conduction constitute the 3-dimensional substrate for atrial fibrillation. Circ Arrhythm Electrophysiol. 2013;6(5):967-75.

90. Lankveld TA, Zeemering S, Crijns HJ, Schotten U. The ECG as a tool to determine atrial fibrillation complexity. Heart. 2014;100(14):1077-84.

91. Narayan SM, Franz MR, Clopton P, Pruvot EJ, Krummen DE. Repolarization alternans reveals vulnerability to human atrial fibrillation. Circulation. 2011;123(25):2922-30.

92. Kim BS, Kim YH, Hwang GS, Pak HN, Lee SC, Shim WJ, et al. Action potential duration restitution kinetics in human atrial fibrillation. J Am Coll Cardiol. 2002;39(8):1329-36.

93. Hiromoto K, Shimizu H, Furukawa Y, Kanemori T, Mine T, Masuyama T, et al. Discordant repolarization alternans-induced atrial fibrillation is suppressed by verapamil. Circ J. 2005;69(11):1368-73.

94. Narayan SM, Bode F, Karasik PL, Franz MR. Alternans of atrial action potentials during atrial flutter as a precursor to atrial fibrillation. Circulation. 2002;106(15):1968-73.

95. Schotten U, Hatem S, Ravens U, Jais P, Muller FU, Goette A, et al. The European Network for Translational Research in Atrial Fibrillation (EUTRAF): objectives and initial results. Europace. 2015;17(10):1457-66.
96. Haissaguerre M, Jais P, Shah DC, Takahashi A, Hocini M, Quiniou G, et al. Spontaneous initiation of atrial fibrillation by ectopic beats originating in the pulmonary veins. N Engl J Med. 1998;339(10):659-66.
97. Arbelo E, Brugada J, Hindricks G, Maggioni AP, Tavazzi L, Vardas P, et al. The atrial fibrillation ablation pilot study: a European Survey on Methodology and results of catheter ablation for atrial fibrillation conducted by the European Heart Rhythm Association. Eur Heart J. 2014;35(22):1466-78.
98. Calkins H, Hindricks G, Cappato R, Kim YH, Saad EB, Aguinaga L, et al. 2017 HRS/EHRA/ECAS/APHRS/SOLAECE expert consensus statement on catheter and surgical ablation of atrial fibrillation. Heart Rhythm. 2017;14(10):e275-e444.
99. Cosedis Nielsen J, Johannessen A, Raatikainen P, Hindricks G, Walfridsson H, Kongstad O, et al. Radiofrequency ablation as initial therapy in paroxysmal atrial fibrillation. N Engl J Med. 2012;367(17):1587-95.
100. Mont L, Bisbal F, Hernandez-Madrid A, Perez-Castellano N, Vinolas X, Arenal A, et al. Catheter ablation vs. antiarrhythmic drug treatment of persistent atrial fibrillation: a multicentre, randomized, controlled trial (SARA study). Eur Heart J. 2014;35(8):501-7.
101. Haissaguerre M, Hocini M, Denis A, Shah AJ, Komatsu Y, Yamashita S, et al. Driver domains in persistent atrial fibrillation. Circulation. 2014;130(7):530-8.
102. Schreiber D, Rieger A, Moser F, Kottkamp H. Catheter ablation of atrial fibrillation with box isolation of fibrotic areas: Lessons on fibrosis distribution and extent, clinical characteristics, and their impact on long-term outcome. J Cardiovasc Electrophysiol. 2017;28(9):971-83.
103. Schreiber D, Rostock T, Frohlich M, Sultan A, Servatius H, Hoffmann BA, et al. Five-year follow-up after catheter ablation of persistent atrial fibrillation using the stepwise approach and prognostic factors for success. Circ Arrhythm Electrophysiol. 2015;8(2):308-17.
104. Scherr D, Khairy P, Miyazaki S, Aurillac-Lavignolle V, Pascale P, Wilton SB, et al. Five-year outcome of catheter ablation of persistent atrial fibrillation using

termination of atrial fibrillation as a procedural endpoint. Circ Arrhythm Electrophysiol. 2015;8(1):18-24.
105. Dong JZ, Sang CH, Yu RH, Long DY, Tang RB, Jiang CX, et al. Prospective randomized comparison between a fixed '2C3L' approach vs. stepwise approach for catheter ablation of persistent atrial fibrillation. Europace. 2015;17(12):1798-806.
106. Hunter RJ, McCready J, Diab I, Page SP, Finlay M, Richmond L, et al. Maintenance of sinus rhythm with an ablation strategy in patients with atrial fibrillation is associated with a lower risk of stroke and death. Heart. 2012;98(1):48-53.
107. Di Biase L, Burkhardt JD, Mohanty P, Mohanty S, Sanchez JE, Trivedi C, et al. Left Atrial Appendage Isolation in Patients With Longstanding Persistent AF Undergoing Catheter Ablation: BELIEF Trial. J Am Coll Cardiol. 2016;68(18):1929-40.
108. Verma A, Macle L, Sanders P. Catheter Ablation for Persistent Atrial Fibrillation. N Engl J Med. 2015;373(9):878-9.
109. Schotten U, Dobrev D, Platonov PG, Kottkamp H, Hindricks G. Current controversies in determining the main mechanisms of atrial fibrillation. J Intern Med. 2016;279(5):428-38.
110. Nishida K, Michael G, Dobrev D, Nattel S. Animal models for atrial fibrillation: clinical insights and scientific opportunities. Europace. 2010;12(2):160-72.
111. Verheule S, Tuyls E, Gharaviri A, Hulsmans S, van Hunnik A, Kuiper M, et al. Loss of continuity in the thin epicardial layer because of endomysial fibrosis increases the complexity of atrial fibrillatory conduction. Circ Arrhythm Electrophysiol. 2013;6(1):202-11.
112. Lin JL, Lai LP, Lin CS, Du CC, Wu TJ, Chen SP, et al. Electrophysiological mapping and histological examinations of the swine atrium with sustained (> or =24 h) atrial fibrillation: a suitable animal model for studying human atrial fibrillation. Cardiology. 2003;99(2):78-84.
113. Linz D, van Hunnik A, Hohl M, Mahfoud F, Wolf M, Neuberger HR, et al. Catheter-based renal denervation reduces atrial nerve sprouting and complexity of atrial fibrillation in goats. Circ Arrhythm Electrophysiol. 2015;8(2):466-74.
114. Morillo CA, Klein GJ, Jones DL, Guiraudon CM. Chronic rapid atrial pacing. Structural, functional, and electrophysiological characteristics of a new model of sustained atrial fibrillation. Circulation. 1995;91(5):1588-95.

115. Gaspo R, Bosch RF, Talajic M, Nattel S. Functional mechanisms underlying tachycardia-induced sustained atrial fibrillation in a chronic dog model. Circulation. 1997;96(11):4027-35.
116. Yue L, Feng J, Gaspo R, Li GR, Wang Z, Nattel S. Ionic remodeling underlying action potential changes in a canine model of atrial fibrillation. Circ Res. 1997;81(4):512-25.
117. Li D, Fareh S, Leung TK, Nattel S. Promotion of atrial fibrillation by heart failure in dogs: atrial remodeling of a different sort. Circulation. 1999;100(1):87-95.
118. Power JM, Beacom GA, Alferness CA, Raman J, Wijffels M, Farish SJ, et al. Susceptibility to atrial fibrillation: a study in an ovine model of pacing-induced early heart failure. J Cardiovasc Electrophysiol. 1998;9(4):423-35.
119. Tanaka K, Zlochiver S, Vikstrom KL, Yamazaki M, Moreno J, Klos M, et al. Spatial distribution of fibrosis governs fibrillation wave dynamics in the posterior left atrium during heart failure. Circ Res. 2007;101(8):839-47.
120. Okuyama Y, Miyauchi Y, Park AM, Hamabe A, Zhou S, Hayashi H, et al. High resolution mapping of the pulmonary vein and the vein of Marshall during induced atrial fibrillation and atrial tachycardia in a canine model of pacing-induced congestive heart failure. J Am Coll Cardiol. 2003;42(2):348-60.
121. Verheule S, Wilson E, Everett Tt, Shanbhag S, Golden C, Olgin J. Alterations in atrial electrophysiology and tissue structure in a canine model of chronic atrial dilatation due to mitral regurgitation. Circulation. 2003;107(20):2615-22.
122. Guerra JM, Everett THt, Lee KW, Wilson E, Olgin JE. Effects of the gap junction modifier rotigaptide (ZP123) on atrial conduction and vulnerability to atrial fibrillation. Circulation. 2006;114(2):110-8.
123. Verheule S, Wilson E, Banthia S, Everett THt, Shanbhag S, Sih HJ, et al. Direction-dependent conduction abnormalities in a canine model of atrial fibrillation due to chronic atrial dilatation. Am J Physiol Heart Circ Physiol. 2004;287(2):H634-44.
124. Ortiz J, Niwano S, Abe H, Rudy Y, Johnson NJ, Waldo AL. Mapping the conversion of atrial flutter to atrial fibrillation and atrial fibrillation to atrial flutter. Insights into mechanisms. Circ Res. 1994;74(5):882-94.
125. Neuberger HR, Schotten U, Verheule S, Eijsbouts S, Blaauw Y, van Hunnik A, et al. Development of a substrate of atrial fibrillation during chronic atrioventricular block in the goat. Circulation. 2005;111(1):30-7.

126. Remes J, van Brakel TJ, Bolotin G, Garber C, de Jong MM, van der Veen FH, et al. Persistent atrial fibrillation in a goat model of chronic left atrial overload. J Thorac Cardiovasc Surg. 2008;136(4):1005-11.
127. Deroubaix E, Folliguet T, Rucker-Martin C, Dinanian S, Boixel C, Validire P, et al. Moderate and chronic hemodynamic overload of sheep atria induces reversible cellular electrophysiologic abnormalities and atrial vulnerability. J Am Coll Cardiol. 2004;44(9):1918-26.
128. Hirose M, Takeishi Y, Miyamoto T, Kubota I, Laurita KR, Chiba S. Mechanism for atrial tachyarrhythmia in chronic volume overload-induced dilated atria. J Cardiovasc Electrophysiol. 2005;16(7):760-9.
129. Ravelli F, Allessie M. Effects of atrial dilatation on refractory period and vulnerability to atrial fibrillation in the isolated Langendorff-perfused rabbit heart. Circulation. 1997;96(5):1686-95.
130. Ninio DM, Saint DA. Passive pericardial constraint protects against stretch-induced vulnerability to atrial fibrillation in rabbits. Am J Physiol Heart Circ Physiol. 2006;291(5):H2547-9.
131. Bode F, Katchman A, Woosley RL, Franz MR. Gadolinium decreases stretch-induced vulnerability to atrial fibrillation. Circulation. 2000;101(18):2200-5.
132. Bode F, Sachs F, Franz MR. Tarantula peptide inhibits atrial fibrillation. Nature. 2001;409(6816):35-6.
133. Hashimoto N, Yamashita T, Tsuruzoe N. Tertiapin, a selective IKACh blocker, terminates atrial fibrillation with selective atrial effective refractory period prolongation. Pharmacol Res. 2006;54(2):136-41.
134. Hashimoto N, Yamashita T, Tsuruzoe N. Characterization of in vivo and in vitro electrophysiological and antiarrhythmic effects of a novel IKACh blocker, NIP-151: a comparison with an IKr-blocker dofetilide. J Cardiovasc Pharmacol. 2008;51(2):162-9.
135. Sinno H, Derakhchan K, Libersan D, Merhi Y, Leung TK, Nattel S. Atrial ischemia promotes atrial fibrillation in dogs. Circulation. 2003;107(14):1930-6.
136. Goldberger AL, Pavelec RS. Vagally-mediated atrial fibrillation in dogs: conversion with bretylium tosylate. Int J Cardiol. 1986;13(1):47-55.
137. Wang Z, Page P, Nattel S. Mechanism of flecainide's antiarrhythmic action in experimental atrial fibrillation. Circ Res. 1992;71(2):271-87.

138. Geddes LA, Hinds M, Babbs CF, Tacker WA, Schoenlein WE, Elabbady T, et al. Maintenance of atrial fibrillation in anesthetized and unanesthetized sheep using cholinergic drive. Pacing Clin Electrophysiol. 1996;19(2):165-75.
139. Mansour M, Mandapati R, Berenfeld O, Chen J, Samie FH, Jalife J. Left-to-right gradient of atrial frequencies during acute atrial fibrillation in the isolated sheep heart. Circulation. 2001;103(21):2631-6.
140. Sarmast F, Kolli A, Zaitsev A, Parisian K, Dhamoon AS, Guha PK, et al. Cholinergic atrial fibrillation: I(K,ACh) gradients determine unequal left/right atrial frequencies and rotor dynamics. Cardiovasc Res. 2003;59(4):863-73.
141. Ono N, Hayashi H, Kawase A, Lin SF, Li H, Weiss JN, et al. Spontaneous atrial fibrillation initiated by triggered activity near the pulmonary veins in aged rats subjected to glycolytic inhibition. Am J Physiol Heart Circ Physiol. 2007;292(1):H639-48.
142. Haugan K, Lam HR, Knudsen CB, Petersen JS. Atrial fibrillation in rats induced by rapid transesophageal atrial pacing during brief episodes of asphyxia: a new in vivo model. J Cardiovasc Pharmacol. 2004;44(1):125-35.
143. Verheule S, Sato T, Everett Tt, Engle SK, Otten D, Rubart-von der Lohe M, et al. Increased vulnerability to atrial fibrillation in transgenic mice with selective atrial fibrosis caused by overexpression of TGF-beta1. Circ Res. 2004;94(11):1458-65.
144. Xiao HD, Fuchs S, Campbell DJ, Lewis W, Dudley SC, Jr., Kasi VS, et al. Mice with cardiac-restricted angiotensin-converting enzyme (ACE) have atrial enlargement, cardiac arrhythmia, and sudden death. Am J Pathol. 2004;165(3):1019-32.
145. Kehat I, Heinrich R, Ben-Izhak O, Miyazaki H, Gutkind JS, Aronheim A. Inhibition of basic leucine zipper transcription is a major mediator of atrial dilatation. Cardiovasc Res. 2006;70(3):543-54.
146. Hagendorff A, Schumacher B, Kirchhoff S, Luderitz B, Willecke K. Conduction disturbances and increased atrial vulnerability in Connexin40-deficient mice analyzed by transesophageal stimulation. Circulation. 1999;99(11):1508-15.
147. Li J, McLerie M, Lopatin AN. Transgenic upregulation of IK1 in the mouse heart leads to multiple abnormalities of cardiac excitability. Am J Physiol Heart Circ Physiol. 2004;287(6):H2790-802.

148. Zhang Z, He Y, Tuteja D, Xu D, Timofeyev V, Zhang Q, et al. Functional roles of Cav1.3(alpha1D) calcium channels in atria: insights gained from gene-targeted null mutant mice. Circulation. 2005;112(13):1936-44.
149. Mancarella S, Yue Y, Karnabi E, Qu Y, El-Sherif N, Boutjdir M. Impaired Ca2+ homeostasis is associated with atrial fibrillation in the alpha1D L-type Ca2+ channel KO mouse. Am J Physiol Heart Circ Physiol. 2008;295(5):H2017-24.
150. Sampson KJ, Terrenoire C, Cervantes DO, Kaba RA, Peters NS, Kass RS. Adrenergic regulation of a key cardiac potassium channel can contribute to atrial fibrillation: evidence from an I Ks transgenic mouse. J Physiol. 2008;586(2):627-37.
151. Temple J, Frias P, Rottman J, Yang T, Wu Y, Verheijck EE, et al. Atrial fibrillation in KCNE1-null mice. Circ Res. 2005;97(1):62-9.
152. Zhang X, Chen S, Yoo S, Chakrabarti S, Zhang T, Ke T, et al. Mutation in nuclear pore component NUP155 leads to atrial fibrillation and early sudden cardiac death. Cell. 2008;135(6):1017-27.
153. Sood S, Chelu MG, van Oort RJ, Skapura D, Santonastasi M, Dobrev D, et al. Intracellular calcium leak due to FKBP12.6 deficiency in mice facilitates the inducibility of atrial fibrillation. Heart Rhythm. 2008;5(7):1047-54.
154. Chelu MG, Sarma S, Sood S, Wang S, van Oort RJ, Skapura DG, et al. Calmodulin kinase II-mediated sarcoplasmic reticulum Ca2+ leak promotes atrial fibrillation in mice. J Clin Invest. 2009;119(7):1940-51.
155. Sah VP, Minamisawa S, Tam SP, Wu TH, Dorn GW, 2nd, Ross J, Jr., et al. Cardiac-specific overexpression of RhoA results in sinus and atrioventricular nodal dysfunction and contractile failure. J Clin Invest. 1999;103(12):1627-34.
156. Ogata T, Ueyama T, Isodono K, Tagawa M, Takehara N, Kawashima T, et al. MURC, a muscle-restricted coiled-coil protein that modulates the Rho/ROCK pathway, induces cardiac dysfunction and conduction disturbance. Mol Cell Biol. 2008;28(10):3424-36.
157. Saba S, Janczewski AM, Baker LC, Shusterman V, Gursoy EC, Feldman AM, et al. Atrial contractile dysfunction, fibrosis, and arrhythmias in a mouse model of cardiomyopathy secondary to cardiac-specific overexpression of tumor necrosis factor-{alpha}. Am J Physiol Heart Circ Physiol. 2005;289(4):H1456-67.
158. Sawaya SE, Rajawat YS, Rami TG, Szalai G, Price RL, Sivasubramanian N, et al. Downregulation of connexin40 and increased prevalence of atrial arrhythmias

in transgenic mice with cardiac-restricted overexpression of tumor necrosis factor. Am J Physiol Heart Circ Physiol. 2007;292(3):H1561-7.
159. Hong CS, Kwon SJ, Cho MC, Kwak YG, Ha KC, Hong B, et al. Overexpression of junctate induces cardiac hypertrophy and arrhythmia via altered calcium handling. J Mol Cell Cardiol. 2008;44(4):672-82.
160. Hong CS, Cho MC, Kwak YG, Song CH, Lee YH, Lim JS, et al. Cardiac remodeling and atrial fibrillation in transgenic mice overexpressing junctin. FASEB J. 2002;16(10):1310-2.
161. Adam O, Frost G, Custodis F, Sussman MA, Schafers HJ, Bohm M, et al. Role of Rac1 GTPase activation in atrial fibrillation. J Am Coll Cardiol. 2007;50(4):359-67.
162. Muller FU, Lewin G, Baba HA, Boknik P, Fabritz L, Kirchhefer U, et al. Heart-directed expression of a human cardiac isoform of cAMP-response element modulator in transgenic mice. J Biol Chem. 2005;280(8):6906-14.
163. Liu F, Levin MD, Petrenko NB, Lu MM, Wang T, Yuan LJ, et al. Histone-deacetylase inhibition reverses atrial arrhythmia inducibility and fibrosis in cardiac hypertrophy independent of angiotensin. J Mol Cell Cardiol. 2008;45(6):715-23.
164. Hirose M, Takeishi Y, Niizeki T, Shimojo H, Nakada T, Kubota I, et al. Diacylglycerol kinase zeta inhibits G(alpha)q-induced atrial remodeling in transgenic mice. Heart Rhythm. 2009;6(1):78-84.
165. Mancia G, Fagard R, Narkiewicz K, Redon J, Zanchetti A, Bohm M, et al. 2013 ESH/ESC guidelines for the management of arterial hypertension: the Task Force for the Management of Arterial Hypertension of the European Society of Hypertension (ESH) and of the European Society of Cardiology (ESC). Eur Heart J. 2013;34(28):2159-219.
166. Costanzo S, Di Castelnuovo A, Zito F, Krogh V, Siani A, Arnout J, et al. Prevalence, awareness, treatment and control of hypertension in healthy unrelated male-female pairs of European regions: the dietary habit profile in European communities with different risk of myocardial infarction--the impact of migration as a model of gene-environment interaction project. J Hypertens. 2008;26(12):2303-11.
167. Beaney T, Schutte AE, Tomaszewski M, Ariti C, Burrell LM, Castillo RR, et al. May Measurement Month 2017: an analysis of blood pressure screening results worldwide. Lancet Glob Health. 2018;6(7):e736-e43.

168. International Consortium for Blood Pressure Genome-Wide Association S, Ehret GB, Munroe PB, Rice KM, Bochud M, Johnson AD, et al. Genetic variants in novel pathways influence blood pressure and cardiovascular disease risk. Nature. 2011;478(7367):103-9.
169. Lifton RP, Gharavi AG, Geller DS. Molecular mechanisms of human hypertension. Cell. 2001;104(4):545-56.
170. Kato N, Takeuchi F, Tabara Y, Kelly TN, Go MJ, Sim X, et al. Meta-analysis of genome-wide association studies identifies common variants associated with blood pressure variation in east Asians. Nat Genet. 2011;43(6):531-8.
171. Vasan RS, Beiser A, Seshadri S, Larson MG, Kannel WB, D'Agostino RB, et al. Residual lifetime risk for developing hypertension in middle-aged women and men: The Framingham Heart Study. JAMA. 2002;287(8):1003-10.
172. Leong XF, Ng CY, Jaarin K. Animal Models in Cardiovascular Research: Hypertension and Atherosclerosis. Biomed Res Int. 2015;2015:528757.
173. Okamoto K, Aoki K. Development of a strain of spontaneously hypertensive rats. Jpn Circ J. 1963;27:282-93.
174. Yan L, Zhang JD, Wang B, Lv YJ, Jiang H, Liu GL, et al. Quercetin inhibits left ventricular hypertrophy in spontaneously hypertensive rats and inhibits angiotensin II-induced H9C2 cells hypertrophy by enhancing PPAR-gamma expression and suppressing AP-1 activity. PLoS One. 2013;8(9):e72548.
175. Welch WJ, Baumgartl H, Lubbers D, Wilcox CS. Renal oxygenation defects in the spontaneously hypertensive rat: role of AT1 receptors. Kidney Int. 2003;63(1):202-8.
176. Klotz S, Hay I, Zhang G, Maurer M, Wang J, Burkhoff D. Development of heart failure in chronic hypertensive Dahl rats: focus on heart failure with preserved ejection fraction. Hypertension. 2006;47(5):901-11.
177. Dahl LK, Heine M, Tassinari L. Role of genetic factors in susceptibility to experimental hypertension due to chronic excess salt ingestion. Nature. 1962;194:480-2.
178. Tian N, Rose RA, Jordan S, Dwyer TM, Hughson MD, Manning RD, Jr. N-Acetylcysteine improves renal dysfunction, ameliorates kidney damage and decreases blood pressure in salt-sensitive hypertension. J Hypertens. 2006;24(11):2263-70.

179. Mullins JJ, Peters J, Ganten D. Fulminant hypertension in transgenic rats harbouring the mouse Ren-2 gene. Nature. 1990;344(6266):541-4.
180. Chung O, Schips T, Rohmeiss P, Gretz N, Strauch M, Unger T. Protein excretion and renal adaptation of transgenic mRen2 rats to changing oral sodium loads. J Hypertens Suppl. 1993;11(5):S188-9.
181. Pinto YM, Buikema H, van Gilst WH, Scholtens E, van Geel PP, de Graeff PA, et al. Cardiovascular end-organ damage in Ren-2 transgenic rats compared to spontaneously hypertensive rats. J Mol Med (Berl). 1997;75(5):371-7.
182. Selye H, Hall CE, Rowley EM. Malignant Hypertension Produced by Treatment with Desoxycorticosterone Acetate and Sodium Chloride. Can Med Assoc J. 1943;49(2):88-92.
183. Chamorro V, Wangensteen R, Sainz J, Duarte J, O'Valle F, Osuna A, et al. Protective effects of the angiotensin II type 1 (AT1) receptor blockade in low-renin deoxycorticosterone acetate (DOCA)-treated spontaneously hypertensive rats. Clin Sci (Lond). 2004;106(3):251-9.
184. Iyer A, Chan V, Brown L. The DOCA-Salt Hypertensive Rat as a Model of Cardiovascular Oxidative and Inflammatory Stress. Curr Cardiol Rev. 2010;6(4):291-7.
185. Klanke B, Cordasic N, Hartner A, Schmieder RE, Veelken R, Hilgers KF. Blood pressure versus direct mineralocorticoid effects on kidney inflammation and fibrosis in DOCA-salt hypertension. Nephrol Dial Transplant. 2008;23(11):3456-63.
186. Kistler PM, Sanders P, Dodic M, Spence SJ, Samuel CS, Zhao C, et al. Atrial electrical and structural abnormalities in an ovine model of chronic blood pressure elevation after prenatal corticosteroid exposure: implications for development of atrial fibrillation. Eur Heart J. 2006;27(24):3045-56.
187. Zeng J, Zhang Y, Mo J, Su Z, Huang R. Two-kidney, two clip renovascular hypertensive rats can be used as stroke-prone rats. Stroke. 1998;29(8):1708-13; discussion 13-4.
188. Wiesel P, Mazzolai L, Nussberger J, Pedrazzini T. Two-kidney, one clip and one-kidney, one clip hypertension in mice. Hypertension. 1997;29(4):1025-30.
189. Henry JP, Liu YY, Nadra WE, Qian CG, Mormede P, Lemaire V, et al. Psychosocial stress can induce chronic hypertension in normotensive strains of rats. Hypertension. 1993;21(5):714-23.

190. Bechtold AG, Patel G, Hochhaus G, Scheuer DA. Chronic blockade of hindbrain glucocorticoid receptors reduces blood pressure responses to novel stress and attenuates adaptation to repeated stress. Am J Physiol Regul Integr Comp Physiol. 2009;296(5):R1445-54.
191. Nishijima Y, Zheng X, Lund H, Suzuki M, Mattson DL, Zhang DX. Characterization of blood pressure and endothelial function in TRPV4-deficient mice with l-NAME- and angiotensin II-induced hypertension. Physiol Rep. 2014;2(1):e00199.
192. Rauchova H, Pechanova O, Kunes J, Vokurkova M, Dobesova Z, Zicha J. Chronic N-acetylcysteine administration prevents development of hypertension in N(omega)-nitro-L-arginine methyl ester-treated rats: the role of reactive oxygen species. Hypertens Res. 2005;28(5):475-82.
193. Xavier F, Magalhaes AM, Gontijo JA. Effect of inhibition of nitric oxide synthase on blood pressure and renal sodium handling in renal denervated rats. Braz J Med Biol Res. 2000;33(3):347-54.
194. Gerdts E, Oikarinen L, Palmieri V, Otterstad JE, Wachtell K, Boman K, et al. Correlates of left atrial size in hypertensive patients with left ventricular hypertrophy: the Losartan Intervention For Endpoint Reduction in Hypertension (LIFE) Study. Hypertension. 2002;39(3):739-43.
195. Gottdiener JS, Reda DJ, Williams DW, Materson BJ, Cushman W, Anderson RJ. Effect of single-drug therapy on reduction of left atrial size in mild to moderate hypertension: comparison of six antihypertensive agents. Circulation. 1998;98(2):140-8.
196. Choisy SC, Arberry LA, Hancox JC, James AF. Increased susceptibility to atrial tachyarrhythmia in spontaneously hypertensive rat hearts. Hypertension. 2007;49(3):498-505.
197. Dunn FG, Pfeffer MA, Frohlich ED. ECG alterations with progressive left ventricular hypertrophy in spontaneous hypertension. Clin Exp Hypertens. 1978;1(1):67-86.
198. Lau DH, Shipp NJ, Kelly DJ, Thanigaimani S, Neo M, Kuklik P, et al. Atrial arrhythmia in ageing spontaneously hypertensive rats: unraveling the substrate in hypertension and ageing. PLoS One. 2013;8(8):e72416.
199. Noresson E, Ricksten SE, Thoren P. Left atrial pressure in normotensive and spontaneously hypertensive rats. Acta Physiol Scand. 1979;107(1):9-12.

200. Pluteanu F, Hess J, Plackic J, Nikonova Y, Preisenberger J, Bukowska A, et al. Early subcellular Ca2+ remodelling and increased propensity for Ca2+ alternans in left atrial myocytes from hypertensive rats. Cardiovasc Res. 2015;106(1):87-97.
201. Kim SJ, Choisy SC, Barman P, Zhang H, Hancox JC, Jones SA, et al. Atrial remodeling and the substrate for atrial fibrillation in rat hearts with elevated afterload. Circ Arrhythm Electrophysiol. 2011;4(5):761-9.
202. Lau DH, Mackenzie L, Kelly DJ, Psaltis PJ, Brooks AG, Worthington M, et al. Hypertension and atrial fibrillation: evidence of progressive atrial remodeling with electrostructural correlate in a conscious chronically instrumented ovine model. Heart Rhythm. 2010;7(9):1282-90.
203. Lau DH, Mackenzie L, Kelly DJ, Psaltis PJ, Worthington M, Rajendram A, et al. Short-term hypertension is associated with the development of atrial fibrillation substrate: a study in an ovine hypertensive model. Heart Rhythm. 2010;7(3):396-404.
204. Fialova M, Dlugosova K, Okruhlicova L, Kristek F, Manoach M, Tribulova N. Adaptation of the heart to hypertension is associated with maladaptive gap junction connexin-43 remodeling. Physiol Res. 2008;57(1):7-11.
205. Spach MS, Boineau JP. Microfibrosis produces electrical load variations due to loss of side-to-side cell connections: a major mechanism of structural heart disease arrhythmias. Pacing Clin Electrophysiol. 1997;20(2 Pt 2):397-413.
206. Yiu KH, Tse HF. Hypertension and cardiac arrhythmias: a review of the epidemiology, pathophysiology and clinical implications. J Hum Hypertens. 2008;22(6):380-8.
207. Eguchi K, Hoshide S, Schwartz JE, Shimada K, Kario K. Visit-to-visit and ambulatory blood pressure variability as predictors of incident cardiovascular events in patients with hypertension. Am J Hypertens. 2012;25(9):962-8.
208. Goette A, Bukowska A, Dobrev D, Pfeiffenberger J, Morawietz H, Strugala D, et al. Acute atrial tachyarrhythmia induces angiotensin II type 1 receptor-mediated oxidative stress and microvascular flow abnormalities in the ventricles. Eur Heart J. 2009;30(11):1411-20.
209. Canpolat U, Oto A, Hazirolan T, Sunman H, Yorgun H, Sahiner L, et al. A prospective DE-MRI study evaluating the role of TGF-beta1 in left atrial fibrosis and implications for outcomes of cryoballoon-based catheter ablation: new insights into

primary fibrotic atriocardiomyopathy. J Cardiovasc Electrophysiol. 2015;26(3):251-9.
210. Goette A, Kalman JM, Aguinaga L, Akar J, Cabrera JA, Chen SA, et al. EHRA/HRS/APHRS/SOLAECE expert consensus on atrial cardiomyopathies: definition, characterization, and clinical implication. Europace. 2016;18(10):1455-90.
211. Verdecchia P, Angeli F, Reboldi G. Hypertension and Atrial Fibrillation: Doubts and Certainties From Basic and Clinical Studies. Circ Res. 2018;122(2):352-68.
212. Vaziri SM, Larson MG, Benjamin EJ, Levy D. Echocardiographic predictors of nonrheumatic atrial fibrillation. The Framingham Heart Study. Circulation. 1994;89(2):724-30.
213. Vaziri SM, Larson MG, Lauer MS, Benjamin EJ, Levy D. Influence of blood pressure on left atrial size. The Framingham Heart Study. Hypertension. 1995;25(6):1155-60.
214. Verdecchia P, Reboldi G, Gattobigio R, Bentivoglio M, Borgioni C, Angeli F, et al. Atrial fibrillation in hypertension: predictors and outcome. Hypertension. 2003;41(2):218-23.
215. Watanabe H, Tanabe N, Makiyama Y, Chopra SS, Okura Y, Suzuki H, et al. ST-segment abnormalities and premature complexes are predictors of new-onset atrial fibrillation: the Niigata preventive medicine study. Am Heart J. 2006;152(4):731-5.
216. Okin PM, Gerdts E, Wachtell K, Oikarinen L, Nieminen MS, Dahlof B, et al. Relationship of left atrial enlargement to persistence or development of ECG left ventricular hypertrophy in hypertensive patients: implications for the development of new atrial fibrillation. J Hypertens. 2010;28(7):1534-40.
217. Medi C, Kalman JM, Spence SJ, Teh AW, Lee G, Bader I, et al. Atrial electrical and structural changes associated with longstanding hypertension in humans: implications for the substrate for atrial fibrillation. J Cardiovasc Electrophysiol. 2011;22(12):1317-24.
218. Schwarzl M, Alogna A, Zweiker D, Verderber J, Huber S, Manninger M, et al. A porcine model of early atrial fibrillation using a custom-built, radio transmission-controlled pacemaker. J Electrocardiol. 2016;49(2):124-31.

219. Schwarzl M, Hamdani N, Seiler S, Alogna A, Manninger M, Reilly S, et al. A porcine model of hypertensive cardiomyopathy: implications for heart failure with preserved ejection fraction. Am J Physiol Heart Circ Physiol. 2015;309(9):H1407-18.
220. Manninger M, Alogna A, Zweiker D, Verderber J, Zirngast B, Adelsmayr G, et al., editors. Increased inducibility of atrial fibrillation in a porcine model of arterial hypertension. Heart Rhythm Society, 36th annual scientific sessions; 2015 May 13th-16th, 2015.
221. Post H, Schmitto JD, Steendijk P, Christoph J, Holland R, Wachter R, et al. Cardiac function during mild hypothermia in pigs: increased inotropy at the expense of diastolic dysfunction. Acta Physiol (Oxf). 2010;199(1):43-52.
222. Schwarzl M, Alogna A, Zirngast B, Steendijk P, Verderber J, Zweiker D, et al. Mild hypothermia induces incomplete left ventricular relaxation despite spontaneous bradycardia in pigs. Acta Physiol (Oxf). 2015;213(3):653-63.
223. Narayan SM, Kazi D, Krummen DE, Rappel WJ. Repolarization and activation restitution near human pulmonary veins and atrial fibrillation initiation: a mechanism for the initiation of atrial fibrillation by premature beats. J Am Coll Cardiol. 2008;52(15):1222-30.
224. Gepstein L, Hayam G, Ben-Haim SA. A novel method for nonfluoroscopic catheter-based electroanatomical mapping of the heart. In vitro and in vivo accuracy results. Circulation. 1997;95(6):1611-22.
225. Bayly PV, KenKnight BH, Rogers JM, Hillsley RE, Ideker RE, Smith WM. Estimation of conduction velocity vector fields from epicardial mapping data. IEEE Trans Biomed Eng. 1998;45(5):563-71.
226. Zeemering S, Maesen B, Nijs J, Lau DH, Granier M, Verheule S, et al. Automated quantification of atrial fibrillation complexity by probabilistic electrogram analysis and fibrillation wave reconstruction. Conf Proc IEEE Eng Med Biol Soc. 2012;2012:6357-60.
227. Muhlfeld C, Nyengaard JR, Mayhew TM. A review of state-of-the-art stereology for better quantitative 3D morphology in cardiac research. Cardiovasc Pathol. 2010;19(2):65-82.
228. Schipke J, Brandenberger C, Rajces A, Manninger M, Alogna A, Post H, et al. Assessment of cardiac fibrosis: a morphometric method comparison for collagen quantification. J Appl Physiol (1985). 2017;122(4):1019-30.

229. Reynolds ES. The use of lead citrate at high pH as an electron-opaque stain in electron microscopy. J Cell Biol. 1963;17:208-12.
230. Mendez J, Keys A. Density and composition of mammalian muscle. Metabolism. 1960;9:184-8.
231. Gundersen HJ, Jensen EB. The efficiency of systematic sampling in stereology and its prediction. J Microsc. 1987;147(Pt 3):229-63.
232. Weibel ER. Stereological Methods. Practical Methods for Biological Morphometry. New York: Academic Press. 1979;1.
233. Geuzaine C, Remacle J-F. Gmsh: a three-dimensional finite element mesh generator with built-in pre- and post-processing facilities. International Journal for Numerical Methods in Engineering. 2009 11:1309-31.
234. Drouhard PV, Roberge FA. Revised formulation of the hodgkin-huxley representation of the sodium current in cardiac cells. Computers and biomedical research, an international journal. 1987 Aug.:333-50.
235. Skouibine KB, Trayanova NA, Moore PK. Anode/cathode make and break phenomena in a model of defibrillation. IEEE transactions on bio-medical engineering. 1999:769-77.
236. Costa CM, Hoetzl E, Rocha BM, Prassl AJ, Plank G. Automatic parameterization strategy for cardiac electrophysiology simulations. Computing in cardiology. 2013:373-6.
237. Miller AW, 2nd, Bohr DF, Schork AM, Terris JM. Hemodynamic responses to DOCA in young pigs. Hypertension. 1979;1(6):591-7.
238. Reil JC, Hohl M, Selejan S, Lipp P, Drautz F, Kazakow A, et al. Aldosterone promotes atrial fibrillation. Eur Heart J. 2012;33(16):2098-108.
239. Sun Y, Ramires FJ, Weber KT. Fibrosis of atria and great vessels in response to angiotensin II or aldosterone infusion. Cardiovasc Res. 1997;35(1):138-47.
240. Brilla CG, Pick R, Tan LB, Janicki JS, Weber KT. Remodeling of the rat right and left ventricles in experimental hypertension. Circ Res. 1990;67(6):1355-64.
241. Rohr S. Arrhythmogenic implications of fibroblast-myocyte interactions. Circ Arrhythm Electrophysiol. 2012;5(2):442-52.
242. Tadic M, Cuspidi C, Ilic I, Suzic-Lazic J, Zivanovic V, Jozika L, et al. The relationship between blood pressure variability, obesity and left atrial phasic function in hypertensive population. Int J Cardiovasc Imaging. 2015.

243. Sun SJ, Yao JL, Xu LB, Rui Q, Zhang NN, Chen M, et al. Cardiac structural remodeling in hypertensive cardiomyopathy. Hypertens Res. 2017;40(5):450-6.
244. Anne W, Willems R, Roskams T, Sergeant P, Herijgers P, Holemans P, et al. Matrix metalloproteinases and atrial remodeling in patients with mitral valve disease and atrial fibrillation. Cardiovasc Res. 2005;67(4):655-66.
245. Dzeshka MS, Lip GY, Snezhitskiy V, Shantsila E. Cardiac Fibrosis in Patients With Atrial Fibrillation: Mechanisms and Clinical Implications. J Am Coll Cardiol. 2015;66(8):943-59.
246. Kostin S, Klein G, Szalay Z, Hein S, Bauer EP, Schaper J. Structural correlate of atrial fibrillation in human patients. Cardiovasc Res. 2002;54(2):361-79.
247. Ohtani K, Yutani C, Nagata S, Koretsune Y, Hori M, Kamada T. High prevalence of atrial fibrosis in patients with dilated cardiomyopathy. J Am Coll Cardiol. 1995;25(5):1162-9.
248. Lie JT, Hammond PI. Pathology of the senescent heart: anatomic observations on 237 autopsy studies of patients 90 to 105 years old. Mayo Clin Proc. 1988;63(6):552-64.
249. Jacquemet V, Henriquez CS. Genesis of complex fractionated atrial electrograms in zones of slow conduction: a computer model of microfibrosis. Heart Rhythm. 2009;6(6):803-10.
250. Eckstein J, Maesen B, Linz D, Zeemering S, van Hunnik A, Verheule S, et al. Time course and mechanisms of endo-epicardial electrical dissociation during atrial fibrillation in the goat. Cardiovasc Res. 2011;89(4):816-24.
251. Burstein B, Nattel S. Atrial fibrosis: mechanisms and clinical relevance in atrial fibrillation. J Am Coll Cardiol. 2008;51(8):802-9.
252. Ausma J, Wijffels M, Thone F, Wouters L, Allessie M, Borgers M. Structural changes of atrial myocardium due to sustained atrial fibrillation in the goat. Circulation. 1997;96(9):3157-63.
253. Boyden PA, Hoffman BF. The effects on atrial electrophysiology and structure of surgically induced right atrial enlargement in dogs. Circ Res. 1981;49(6):1319-31.
254. Zou R, Kneller J, Leon LJ, Nattel S. Substrate size as a determinant of fibrillatory activity maintenance in a mathematical model of canine atrium. Am J Physiol Heart Circ Physiol. 2005;289(3):H1002-12.

255. Milliez P, Girerd X, Plouin PF, Blacher J, Safar ME, Mourad JJ. Evidence for an increased rate of cardiovascular events in patients with primary aldosteronism. J Am Coll Cardiol. 2005;45(8):1243-8.
256. Rossi GP, Cesari M, Cuspidi C, Maiolino G, Cicala MV, Bisogni V, et al. Response to Effectiveness of adrenalectomy and aldosterone antagonists for long-term treatment of primary aldosteronism. Hypertension. 2013;62(4):e14.
257. Swedberg K, Zannad F, McMurray JJ, Krum H, van Veldhuisen DJ, Shi H, et al. Eplerenone and atrial fibrillation in mild systolic heart failure: results from the EMPHASIS-HF (Eplerenone in Mild Patients Hospitalization And SurvIval Study in Heart Failure) study. J Am Coll Cardiol. 2012;59(18):1598-603.